UCRL-53251
Distribution Category UC-70

UCRL--53251

DE82 017119

Instrumentation Report No. 2: Identification, Evaluation, and Remedial Actions Related to Transducer Failures at the Spent-Fuel Test—Climax

W. C. Patrick

R. C. Carlson

N. L. Rector

Manuscript Date: November 30, 1981

LAWRENCE LIVERMORE LABORATORY
University of California • Livermore, California • 94550

Available from: National Technical Information Service • U.S. Department of Commerce
5285 Port Royal Road • Springfield, VA 22161 • $7.00 per copy • (Microfiche $3.50)

INSTRUMENTATION REPORT NO. 2: IDENTIFICATION, EVALUATION, AND REMEDIAL ACTIONS RELATED TO TRANSDUCER FAILURES AT THE SPENT FUEL TEST--CLIMAX

ABSTRACT

The Spent Fuel Test-Climax (SFT-C) is a test of the feasibility of safe and reliable short-term storage and retrieval of spent fuel from commercial nuclear reactors. In support of operational and technical goals of the test, about 850 channels of instrumentation have been installed at the SFT-C.

Failure of several near-field instruments began less than six months after emplacement of 11 canisters of spent fuel and activation of six thermally similar simulators. The failed units were linear potentiometers (used to make displacement measurements) and vibrating wire stressmeters (used to make change-in-stress measurements). This report discusses the observed problems and remedial actions taken to date.

INTRODUCTION

The Lawrence Livermore National Laboratory (LLNL) is conducting a test of the feasibility of safe and reliable short-term storage and retrieval of spent fuel from commercial reactors. This test, known as the Spent Fuel Test-Climax (SFT-C), is a part of the Nevada Nuclear Waste Storage Investigations of the U.S. Department of Energy (DOE).[1]

The SFT-C test level is 420 m below surface in a granite intrusive on the DOE Nevada Test Site (NTS). Eleven spent fuel assemblies, six electrical simulators, and twenty peripheral guard heaters are simulating the near-field effects of a large-scale repository. The effect of this simulation is to raise ambient air and rock temperatures from about 23°C to as much as 32°C and 85°C, respectively.[2] The SFT-C was planned as a 3- to 5-year test,[1] and consideration was given to selecting instruments which would survive a hostile environment for that period of time.[3]

Less than six months after spent fuel emplacement began, failures of several near-field instruments were observed. Since these units were purchased 15 months earlier, they were no longer under the manufacturer's one-year warranty. Failures of linear potentiometers occurred on canister drift extensometers located 1.4 to 2.0 m from the heat sources, along with failures of vibrating-wire stressmeters emplaced about 1 m from the heat sources.

This report documents the evaluation of failures and the remedial actions taken to restore the data acquisition capabilities of both instrument types. For completeness, we present a brief description of the instruments, installation procedures, and a history of the identification of the failures. The report is organized by instrument type, and each of the topics mentioned is discussed for the particular instrument and its failure.

The reported instrument failures are significant because many field tests are planned or are in progress, both in the United States and in other countries. In addition, monitoring equipment will likely be emplaced in the early stages of a repository. Such instrumentation will need to function in hostile environments for years or decades. Because this issue is important and there is general interest in results at the SFT-C, we have modified the SFT-C test plan to include instrument evaluation as an objective.

ROD EXTENSOMETER TRANSDUCER FAILURES

Extensometers of various types are used throughout the SFT-C.[4] The type of linear potentiometer which has failed is deployed in 14 four-anchor units in the canister drift (56 total), 12 three- and six-anchor units in the heater drifts (60 total), 7 three-component fracture monitors (21 total), 16 two-component convergence wires (32 total), and 2 one-component convergence wires (2 total). Failures to date have been limited to the first named units. Of 56 transducers present, 23 (i.e., 41%) have failed.

INSTRUMENT AND TRANSDUCER DESCRIPTION

The GxE-series* rod extensometers deployed at the SFT-C are standard Terrametrics units with a few special features.[3] The standard hydraulic anchors, without check valves, associated with each measurement point have been coupled to a nitrogen over DTE-25 hydraulic oil-pressure maintenance system. Invar rather than mild steel has been used for the rods to minimize thermal effects. Even so, thermocouples are located at each hydraulic anchor to facilitate correction for thermal expansion.

Assembling the mechanical components of the rod extensometers took place in the central canister drift of the SFT-C (see Fig. 1). Invar rods were

* Throughout this report, lower case x is used to indicate generalization of a series of designators, (e.g., GxE for GAE, GBE, GCE, and GDE together).

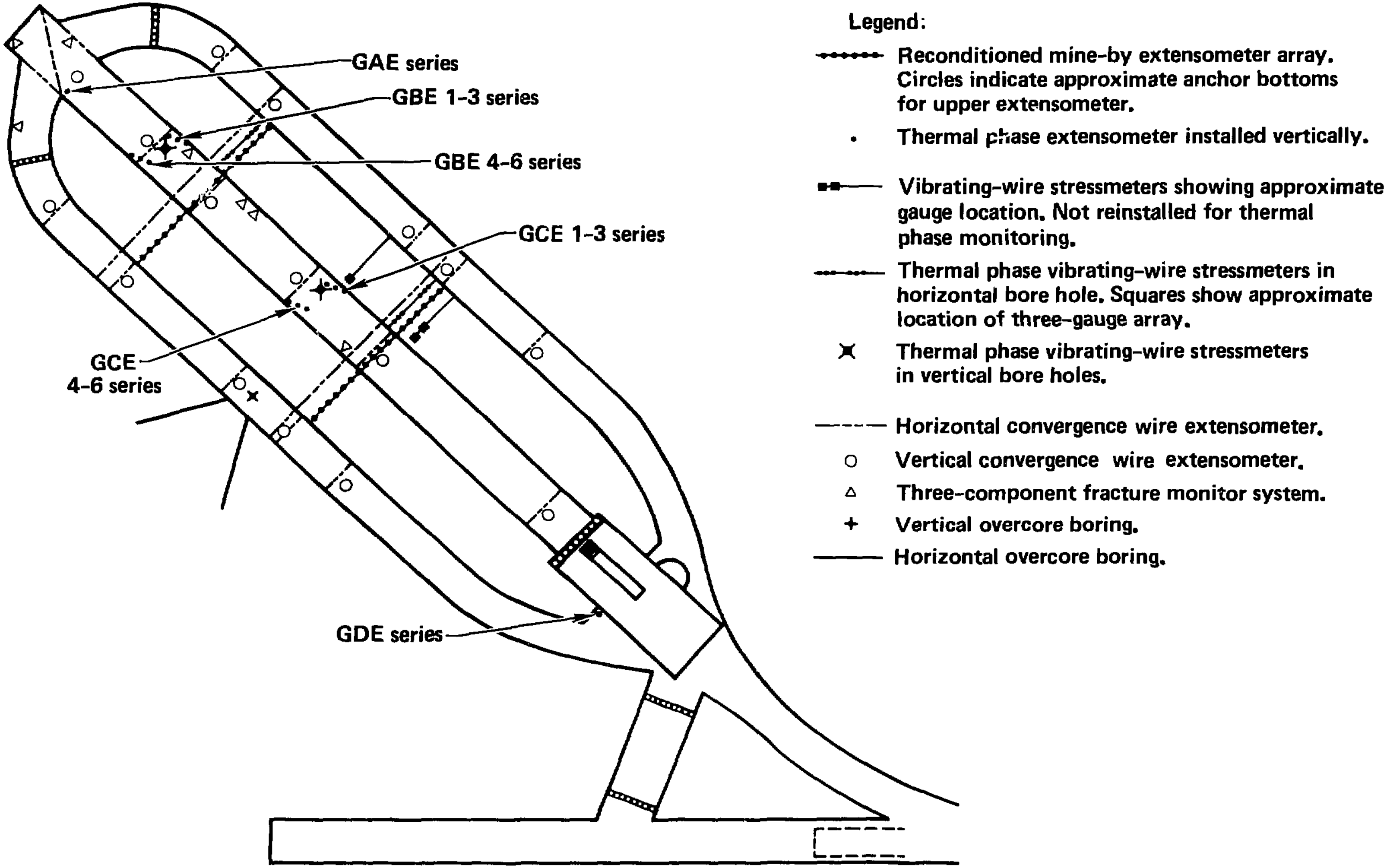

FIG. 1. Plan view of geotechnical instrumentation for heated phase of SFT-C.

screwed into mating hydraulic anchors, thermocouples were attached to the interior of each anchor with a few drops of Hardman Epoxiweld, and the assembly was sheathed in silicone-rubber-shielded flexible conduit. Assembled units were placed in their respective 76 mm diam (NX) boreholes and left there for 24 to 56 days, until all units were assembled and grouting equipment was available.

The holes in which the units were placed were generally dry. The few which contained several centimetres of water were blown dry with compressed air. Although the test level is above the regional water table, some water is present in fractures and accumulates in the bottom of some drill holes. During grouting, this accumulated water was displaced out the top of the hole by the grout.

Immediately after grouting, the anchors were pressurized and the grout was allowed to cure. Installation of extensometer head assemblies and associated transducers began several days after the grouting operation.

The rod extensometer transducer circuit is shown in Fig. 2. The potentiometers are Bourns Model 5184 (5 kΩ ± 10%, 25-mm stroke units). These units feature infinite resolution by means of a resistive polymer element. In this configuration, the ratio of output voltage to excitation is linear with respect to the position of the potentiometer wiper. Output voltage is 0.0 at the wiper center position as a result of the precision Visnay 2.5 kΩ resistors in the circuit.

Total resistance (RT) of each potentiometer was measured on receipt of the transducer at LLNL or EG&G Atlas. All units were within the resistance specification of ±10%. To establish calibration curves, linearity, and hysteresis, calibration was performed in the laboratory over the full range of each potentiometer. Then transducers were installed and field calibrated over the central 5 mm of wiper travel. All units were within linearity and hysteresis specification on receipt with the exception of a few which required additional washers to reduce backlash or polishing of the shaft to reduce activation force.

SUMMARY HISTORY AND IDENTIFICATION OF PROBLEM

Computer-recorded readings of relative displacement at one extensometer (GCE023) began to be significant in late August 1980 (see Fig. 3). The recorded displacements caused no concern since they were reasonable by at

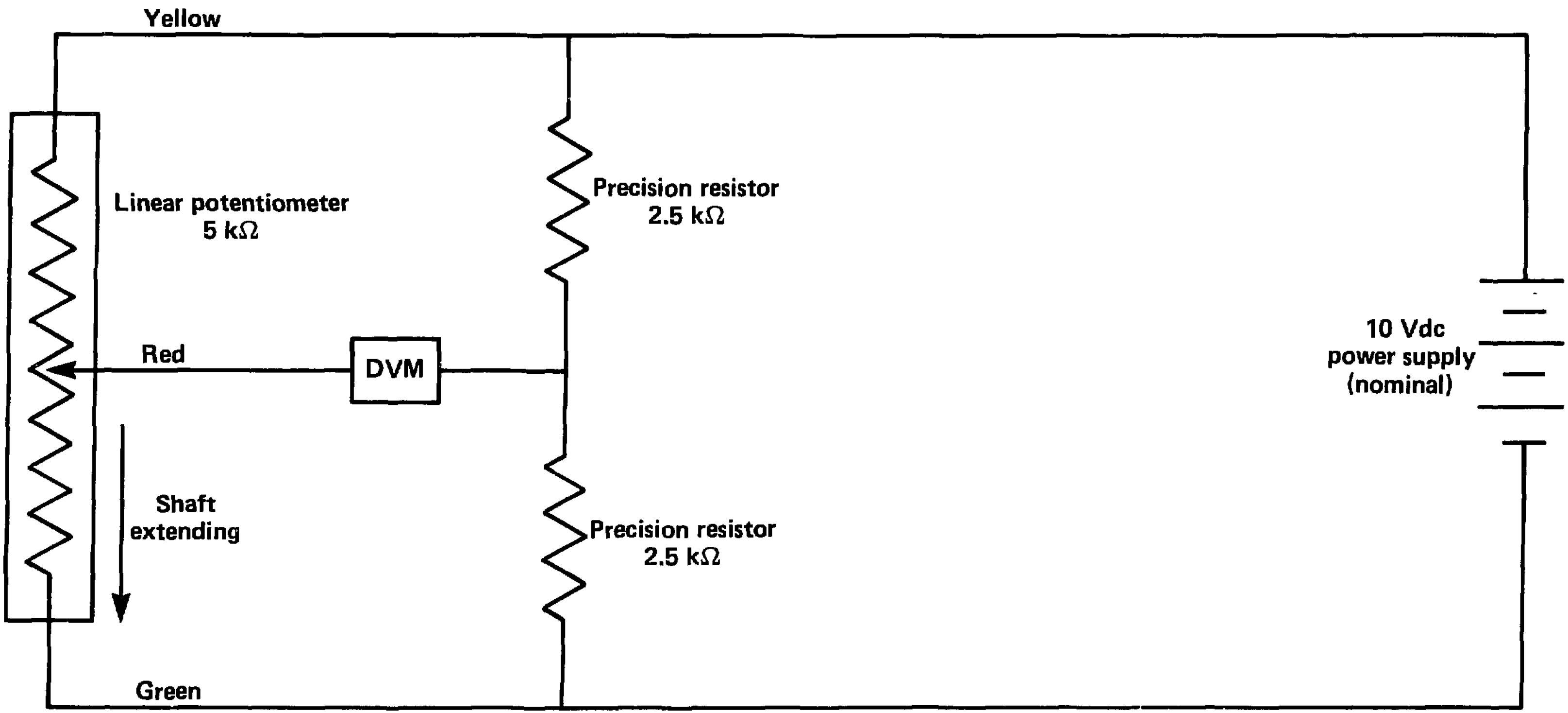

FIG. 2. Schematic of the transducer electrical circuit using linear potentiometer.

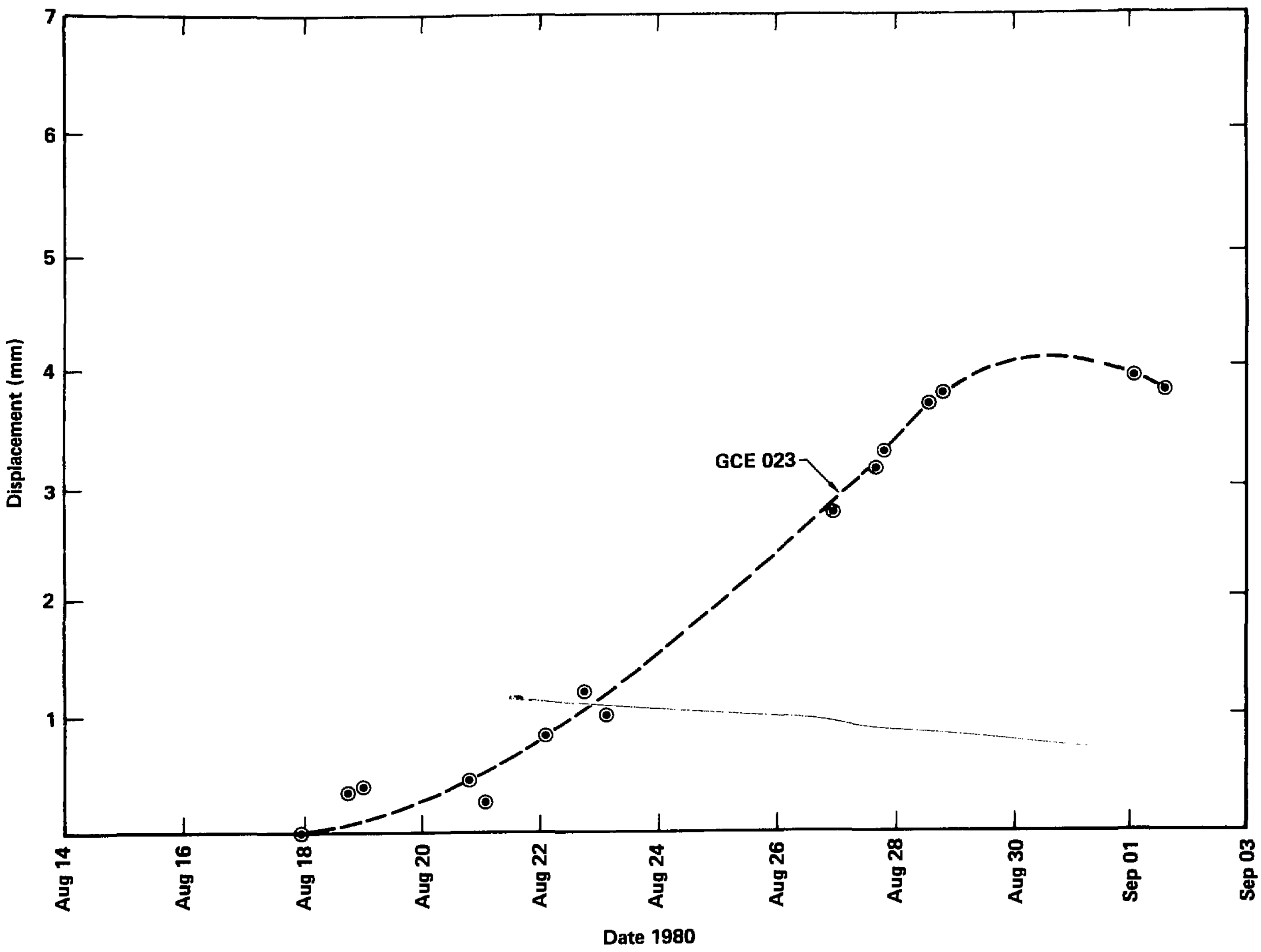

FIG. 3. Preliminary data plots.

least three criteria. First, they were in the correct direction for early-time displacements in that they reflected relative compression between the anchor point and the head assembly, reflecting thermal expansion and upward motion of the rock near the anchor. Second, they were in the range of expected displacements. Third, they were following a familiar S-shaped response curve.

In early September, routine monitoring showed other units responding in similar fashion (e.g., GCE014, GBE013, GCE033, and GCE063). Apparent displacements became large enough (i.e., over 5 mm) to provoke concern, and a field inspection of these units took place. This inspection revealed that although the data acquisition system was recording voltages indicative of several millimetres of displacement, the potentiometer shaft had not moved relative to the potentiometer body.

Voltage measurements at the instrument head revealed that the problem was located there, not in the data acquisition system hardware or software. A further set of voltage measurements and confirming resistance measurements indicated that the resistance of the potentiometers was changing with time and the changes were nonlinear.

A series of field and laboratory tests then were undertaken, which are described later and which indicated the possibility of chemical vapor action on the potentiometer resistive element. Based on this assessment, the head assembly covers were removed to vent such vapors.

Replacement Bourns potentiometers were ordered, received, and calibrated at EG&G Atlas. About two weeks later, samples of the units were checked for RT, and several were found to be out of specification. In all, 21 (i.e., 33%) of the 64 replacement units failed, all with linear changes in RT (see Appendix C).

As will be discussed later, a second series of laboratory tests were undertaken, and close interaction with Bourns personnel insued. Failures were found to have the characteristics of large, linear changes in RT, a marked difference from earlier nonlinear failures observed in the field.

Further investigations led to eliminating several possible causes of failure; however a totally satisfactory answer to the problem has not been found to date. A decision has now been made to retrofit the GBE- and GCE-series extensometers with new transducers. These 12 four-component units have received four types of transducers in equal numbers: (1) Bourns rectilinear potentiometers, (2) Vernitron rectilinear potentiometers, (3) KAMAN proximeters, and (4) Schaevitz linear variable differential transformers.

EVALUATION OF FAILURES

Once a problem of instrument reliability had been identified, a series of field and laboratory tests were undertaken to determine the extent and cause of the observed problems. This investigation included field measurements of component characteristics, gas sampling, and laboratory testing over a range of temperatures and humidities.

Field Measurements

When the recorded displacements became suspiciously large, field measurements were made by the authors to ascertain the validity of the acquired data. The head assembly containing GCE021-024 was isolated from the Data Acquisition System (DAS), and voltage measurements were made between the potentiometer wiper and the center connection of the precision bridge resistors (see Fig. 2). Voltage drops of -0.0687, -0.4507, +2.772, and -0.4853 were recorded for GCE021-024, respectively. These voltages correspond to -0.1745, -1.145, 7.041, and -1.233 mm, respectively. Despite this marked difference between GCE023 and the remaining three units on the same head assembly, the lengths of the shafts protruding from the potentiometer cases were essentially the same. A resistance measurement showed that the nominal 5 kΩ unit now had a resistance of about 6.5 kΩ that was nonlinear along the element. Clearly, this one unit was no longer functional.

A series of simultaneous resistance and shaft-length measurements were performed to determine the magnitude of the observed problem. Appendix A presents the results of these measurements together with the pre-installation total-resistance measurements. In summary, 23 (i.e., 41%) of all units were found to have RT outside the 5 kΩ ± 10% limits specified at the time of purchase. Of the 23, 21 were out of specitication on the high side and 2 were out of specification on the low side of the range. Changes in RT between November 13, 1979, and November 19, 1980, averaged 46% on units which were out of specification on November 19, 1980, and 5% on units which were in specification on this date. Since linear changes in resistance would not adversely affect displacement measurements, shaft length measurements were made to provide a rough check on actual displacement. Shaft lengths averaged 16.8 ± 0.457 mm, a variation of ± 2.7%. We could imply, then, that all units had been displaced nearly the same amount; yet, the resistance measurements indicated a broad range of displacements. Nonlinear changes in the potentiometer resistive elements were the apparent cause of the transducer failures.

At this point, only transducers associated with the G-series extensometers in the canister drift had exhibited failures. Since 171 transducers of the same design and manufacture were deployed in four similar applications at the SFT-C, determining the extent of failures was an important concern. Measurement of RT on the 115 transducers associated with MBI-, FMS-, CWE-, and THE-series instruments revealed that all were within specification although minor changes in RT (generally, <100 Ω) had occurred since installation. Appendix B presents the results of these measurements. As was noted previously, minor linear changes have been observed in other installations and are known not to influence the performance of these transducers.

In the early field analysis, two of the Vishay precision bridge-completion resistors were found to be slightly out of specification (GBE030 and GCE030). X-ray analysis indicated void defects in the resistive elements. The failures were limited to these two observations, and no relationship with potentiometer failures was established. At the suggestion of the manufacturers, these units were replaced with hermetically sealed units.

Failure Hypotheses

Having observed the limited extent of the transducer failures, we began to develop a table of those instrument characteristics and conditions which may have contributed to the failure of some transducers but not others. We developed this failure analysis matrix (see Table 1) over the course of several weeks, as testing continued. The replacement potentiometers for the G-series extensometers are also included in the table, although they have not yet been discussed.

During the course of this investigation, seven failure hypotheses were considered in light of data available at the time. Several of these were quite easily dismissed, while others required significant testing. Typically, more than one failure hypothesis was under consideration at a given time.

Table 1. Potentiometer failure analysis matrix.

Condition	Instrument series: GxE	GxE replacement	CWE	FMS	MBI
1. Current status	Nonlinear changes in total resistance	Linear changes in total resistance	OK	OK	OK total
2. Status on receipt	OK	OK	OK	OK	OK
3. Laboratory doing calibration	EG&G[a]	EG&G[a]	LLNL[b]	LLNL[b]	Terrametrics and EG&G[a]
4. Serial numbers	3578,3978,4078	1780,4480,4880 5280,0581	0680	0680	3478,3578, 3678,3978
5. Orientation	+90° (vert)	0° (hor)	+90°	Various: ±90°	0°, -33°, -50°,
6. Transducer temperature (°C)	25 to 32	23 to 27	25 to 32	25 to 32	25 to 32
7. Instrument temperature (°C)	40 to 60	N/A	25 to 32	25 to 32	25 to 32
8. Transducer enclosure	0-ring sealed	None	None	None	Some 0-ring sealed
9. Shock and vibration	Infrequent (<0.1 g)	None	Infrequent (<0.1 g)	Infrequent (<0.1 g)	Infrequent (≤100 g)

[a] EG&G, Inc., Las Vegas, NV.
[b] Lawrence Livermore National Laboratory, Livermore, CA.

Hypothesis 1. The first hypothesis was that the failures came from a bad batch. This was dismissed because the failing units in the GxE-series came from the same lots as did the MBI-series where no failures had been observed (see Table 1, item 4).

Hypothesis 2. Before field measurements of RT were made on the MBI-series potentiometers, a relationship existed between failures and the laboratory which performed the calibrations (see Table 1, item 3). This hypothesis was dismissed when the field measurements were made.

Hypothesis 3. Also considered was the potential for electrical damage caused by overpowering the units. Records of excitation voltage (10.5 Vdc) and the configuration of the circuit indicate that elevated power conditions did not occur during the test.

Hypothesis 4. Two potential sources of direct mechanical damage were evaluated qualitatively. Excess wear of the resistive element is highly unlikely since none of the potentiometers would have been cycled more than 10 times during calibration. Furthermore, the application is quasistatic; i.e., no dithering is experienced.

Hypothesis 5. Damage by shock loading is most likely to be present in the MBI-series units which were subjected to explosive loading during excavation of the facility (see Table 1, item 9). All other instruments have experienced only low-g, long-period, infrequent shocks from nuclear weapons tests at the site.[5]

Hypothesis 6. No relationship was found between transducer temperature (see Table 1, item 6) and failure, but an indirect relationship is seen between the temperature of the downhole portion of the instrument and failure (see Table 1, item 7). This relationship led to some of the most extensive testing. It is conceivable that elevated temperatures down-hole could have generated and transported vapors which, being trapped in the O-ring sealed head assembly, could have damaged the potentiometer resistive element. A potential source of vapors was acetic acid produced during the curing of silicone rubber sealing agents. Tests aimed at confirming the hypothesis of chemical vapor damage are discussed in following sections.

Hypothesis 7. Another intriguing hypothesis deals with variations in hygroscopic affects along resistive elements. The manufacturer stated that the resistive material is hygroscopic; i.e., it absorbs available moisture. Since this material is coated with silicone oil at manufacture, it is initially sealed. With time, the oil on the upper part of the vertically-oriented element could flow downward, exposing part of the element to available moisture. Since resistance was known to increase with the absorption of moisture and since 21 of the 23 failed units showed increases in resistance on the upper portion of the potentiometer, the hypothesis of differential hygroscopy appeared to be reasonable.

Further testing, described in the following sections, was aimed principally at confirming or rejecting the two leading hypotheses of potentiometer failure: (1) degradation of the resistive element by chemical vapor action and (2) differential hygroscopy of the resistive element.

Gas Sampling

During the initial field inspection of GCE023, the authors noticed an acetic acid odor when the protective cap of the head assembly was removed. Although acetic acid was present as a curing product of RTV compounds used in sealing downhole components of the extensometers, two factors limited the likelihood of the vapor being present. First, the RTV was applied only to the outside of the assembled components. Second, the assembled extensometers hung in their respective emplacement holes for several weeks before being anchored and grouted in place. This should have allowed for adequate curing of the RTV.

In an effort to confirm the presence of acetic acid, which is known to adversely affect electronic components, gas sampling was performed at several head assemblies when the head assembly covers were first removed. The results of mass spectrometric analyses of these samples are shown in Table 2. Several sample bottles were heated to revaporize condensed liquids. The analyses remained the same. All organic compounds present were in insufficient quantities to permit analysis. A comparison of GAE, GDE, and MBI results, where no failures have occurred, with GBE and GCE results, where all failures have occurred to date, is inconclusive. The presence and concentrations of the several gases include both failed and good extensometer units. We must conclude that acetic acid or any organic compound, if present, is below the limits of detectability for the equipment used in these analyses.

Table 2. Summary of analyses of gas obtained from extensometer head assemblies.

Instrument No.	Concentration of Compound (volume percentage) N2	O2	Ar	CO2	H2	Comments
GAE-1	80.54	18.42	0.935	0.089	0.012	CO_2 and H_2 high, trace organics
GBE-1	79.59	19.41	0.945	0.046	0.016	H_2 high, trace organics
GBE-2	79.44	19.55	0.935	0.042	0.026	H_2 high, trace organics
GBE-3	82.02	16.90	0.961	0.043	0.069	H_2 high, trace organics
GBE-4	80.64	18.32	0.943	0.064	0.032	CO_2 and H_2 high, trace organics
GBE-5	80.03	18.97	0.932	0.053	0.022	H_2 high, trace organics
GBE-6	80.61	18.35	0.961	0.055	0.023	H_2 high, trace organics
GCE-1	78.51	20.50	0.930	0.054	ND[a]	Normal
GCE-2	78.66	20.37	0.916	0.053	ND[a]	Normal
GCE-4	80.91	18.03	0.954	0.048	0.049	H_2 high, trace organics
GCE-5	80.23	18.74	0.942	0.049	0.038	H_2 high, trace organics
GCE-6	80.29	18.67	0.941	0.058	0.036	CO_2 and H_2 high, trace organics
GDE-1	79.13	19.87	0.941	0.050	0.011	H_2 high, trace organics
MBI-1	78.54	20.45	0.929	0.068	ND[a]	CO_2 high
MBI-4	78.49	20.52	0.934	0.057	ND[a]	Normal
MBI-5	78.65	20.31	0.934	0.101	ND[a]	CO_2 high, trace organics
MBI-8	78.65	20.37	0.920	0.053	ND[a]	Normal
MBI-11	78.52	20.42	0.926	0.119	0.012	CO_2 and H_2 high, trace organics

[a] ND = Not detectable.

Hygroscopy Studies

Hygroscopy studies were undertaken to test the hypothesis that nonlinear changes in potentiometer resistance could be the result of differential absorption of moisture along the resistive element. These tests used vacuum and elevated temperature in an attempt to reverse the observed changes. These methods are alternative ways of driving off moisture. The first series of tests utilized potentiometers from the original G-series instruments which had exhibited nonlinear changes in RT.

Initial tests on the original G-series potentiometers were performed in a bell jar. Temperature was ambient (25°C) and vacuum was achieved by a roughing pump (25 to 30 mm Hg). Under these conditions, the RT of number 3578-375 was decreased from 9907 to 9691 Ω, about 2.2%. This decrease was evenly divided between the upper (2.4% change) and lower (1.6% change) halves of the resistive element. Upon release of the vacuum, we found that the RT was about 2% higher than the pretest value. Further tests with this and three other potentiometers produced the results shown in Table 3. We conclude that either vacuum or elevated temperature can produce minor decreases in total resistance of the potentiometers. As in the initial test, these changes are divided in roughly equal proportions in the upper and lower sections of the resistive elements. This implies that only linear changes in resistance are induced by humidity in these transducers.

Table 3. Summary results of elevated temperature and vacuum testing of original G-series potentiometers.

Test Conditions	Potentiometer Serial No. 3578-364	3578-372	3578-375	3978-561
Pretest total resistance at 25°C and 1 atm (Ω).	6305	7362	10090	5559
Change induced by 15 µm vacuum (%)	-3.7	-3.4	-4.1	-4.0
Change induced by 100°C heating for 34 h (%)	-2.7	N/A	-19.4	N/A
Final total resistance at 25°C and 1 atm (Ω).	6361	7444	9147	5579

Since the mode of failure in the replacement G-series potentiometers was linear, additional tests at vacuum and elevated temperature were performed on several of these transducers. Table 4 summarizes the results of these tests. Several interesting observations can be made from these results. First and most importantly, items 2, 4, and 5 show that fairly significant changes in RT can be induced and maintained by first subjecting the potentiometer to elevated temperature and then inserting again into its case prior to cooling. The reduced RT values were maintained for three to four days during the test. These changes appear to be linearly distributed along the resistive element and roughly proportional to RT. No change was sufficient to return a potentiometer to specification. Second, subjecting the potentiometers to vacuum initially decreased the RT, but it returned to about the pretest level almost immediately after its return to atmospheric pressure (item 1). Item 3 provides the interesting result indicating that heating the transducer while it is encased actually produces an increase in RT over its preheated value.

We conclude from the hygroscopy studies that although some reduction in RT (i.e., 2.7 to 11.2%) can be induced and maintained by reducing the available moisture, such changes are too small to return a potentiometer which is out of specification to an acceptable value. The observed reductions are apparently linear whether the potentiometer failed in a linear or a nonlinear mode. This evidence leads us to conclude that hygroscopy of the potentiometer resistive element is not the primary cause of either observed mode of failure.

Miscellaneous Supporting Tests

Several tests were performed either to address established failure hypotheses or to probe for additional failure mechanisms. These included optical inspection, chemical softening, and X-ray diffraction.

Optical inspection of the resistive elements of several potentiometers was performed at various level of magnification. Four of the original G-series transducers, having a broad range of RT, were found to have ripples and dimples ("orange-peel effect") in the resistive elements. With few exceptions, there was an apparent increase in this effect with increasing RT. One transducer, 3578-366, had a roughened, raised area in the resistive element which chipped when the wiper assembly was cycled over it (see Fig. 4). This unit had the largest observed RT, about 20 kΩ. Three of the replacement G-series transducers exhibited smooth, flat resistive elements

Table 4. Summary results of elevated temperature and vacuum testing of replacement G-series potentiometers.

Test conditions	Potentiometer Serial No. 4078-009 (Ω)	(%)	4480-452 (Ω)	(%)	4480-456 (Ω)	(%)
1. Pretest RT at 25°C and 1 atm	5418		5817		6486	
Low RT at 25°C and 25 μm	5243	-3.2	5507	-5.3	6046	-6.8
RT after return to 1 atm, gauge out of case	5416	-0.0	5823	+0.1	6449	-0.6
2. Low RT after heating at 50°C, out of case	5124	-5.4	5341	-8.2	5774	-11.0
RT after return to 25°C, encased before removal from oven	5228	-3.5	5506	-5.4	5938	-8.4
3. Low RT after reheating at 50°C, in case during and after heating	N/A		N/A		5794	-10.7
RT after return to 25°C, in case	N/A		N/A		5992	-7.6
4. Low RT after reheating at 50°C, out of case	N/A		N/A		5598	-13.7
RT after return to 25°C, encased before removal from oven	N/A		N/A		5762	-11.2
5. Post-test at 25°C and 1 atm	5256		5566		5762	
Net change in RT	162	-3.0	251	-4.3	724	-11.2

under the same inspection. The observed relationships indicate that rough surface texture (1) is at least associated with, (2) is probably a symptom of, and (3) may be a cause of the observed nonlinear failures. The causative status cannot be verified because the potentiometers were not subjected to an

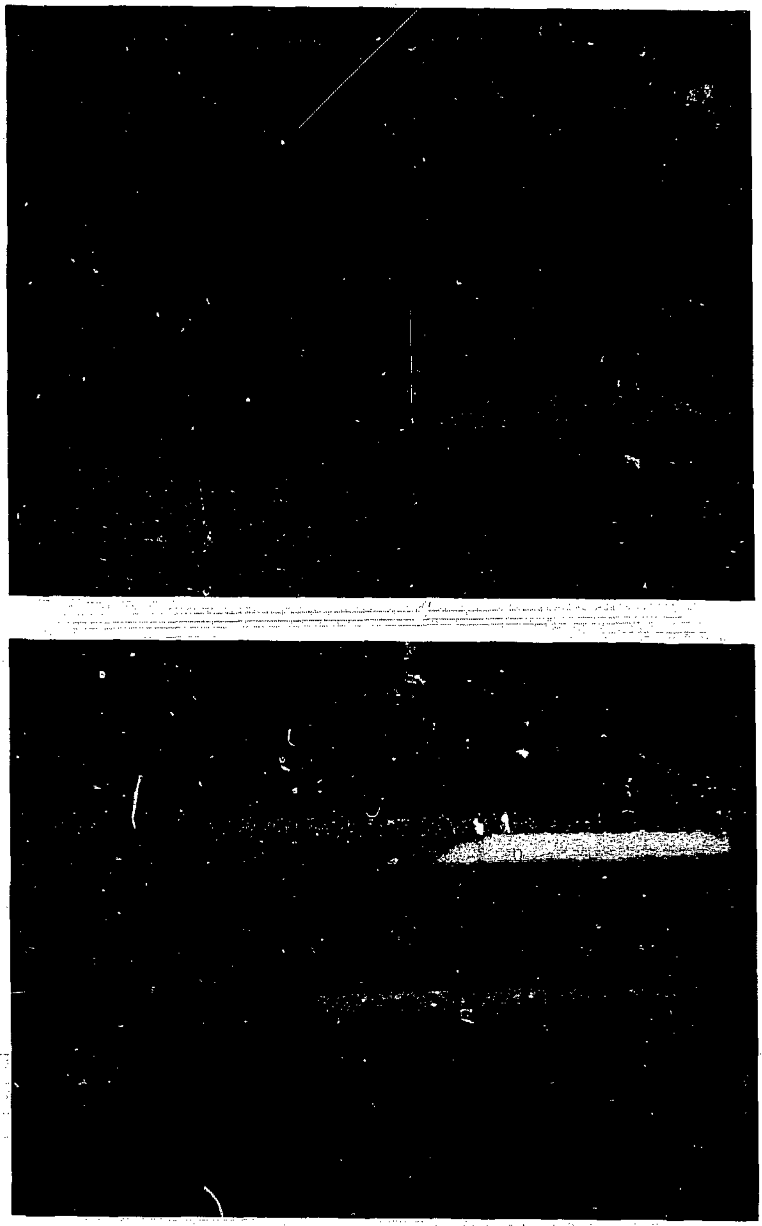

FIG. 4. Photomicrographs showing debonded, abraded section of resistive element.

optical inspection at receipt, since this would have required disassembly of the units.

The susceptibility of the resistive elements to chemical attack was tested using two powerful industrial solvents which are used in the plastics industry. Bourns describes the resistive material as a "conductive plastic electrical element." After an initial dip test indicated no deterioration, two samples were soaked in Kenstrip 902 for 20 h and ethylene dichloride for 21 h, respectively. At the end of this period, no noticeable dissolution or softening of the resistive elements had occurred. We conclude that, provided it actually is a plastic, the resistive element is not susceptible to degradation by these two chemical solvents.

Small amounts of rust were observed in the protective caps of the rod extensometer head assemblies. X-ray diffraction analyses of this material were performed to determine whether its chemistry would provide additional insight into the hypothesized presence of chemical vapors in the head assembly. The analyses showed that the material was hematite, Fe_2O_3, and lepidocrocite, FeO(OH), two common rusts. No positive evidence of unusual chemical corrosion of the head assemblies was obtained from these tests.

Chemical Interaction Test

Most of the foregoing tests were aimed at finding evidence of an irreversible process (e.g., chemical damage) or correcting a reversible process (e.g., hygroscopic effects). A final test was directed toward causing the hypothesized damage of the resistive element by exposure to acetic acid.

This test was conducted by first thoroughly cleaning the resistive element of a potentiometer from the replacement G-series, Serial No. 4078-013. Half of the resistive element was then coated liberally with silicone oil to provide some degree of protection for this surface. The prepared potentiometer was placed in a bell jar enclosure with an open bottle of glacial acetic acid, and resistance measurements were made over a period of 25 days. At the end of this period, RT had increased 1227 Ω (24.2%). This increase was distributed over the silicone-oil coated and uncoated ends of the potentiometer fairly linearly, i.e., 600 Ω (25.7%) and 642 Ω (22.9%), respectively.

The potentiometer was removed from the test chamber and allowed to remain at ambient temperature and air quality for 35 days. Total resistance decreased to 5408 Ω. This is within specification for these units but is still about 6.8% above the pretest value of RT. However, data in Appendix C shows that the current value of RT is only 1.6% above that recorded on 21 April 1981. This test indicates that damage induced by acetic acid is reversible and, therefore, probably is not the cause of the observed irreversible changes in RT.

REMEDIAL ACTIONS

The basic approach in taking remedial actions on the failed potentiometers was to diverge from the original philosophy of installing only off-the-shelf instrumentation.[3] A period of instrument evaluation is now planned for the remaining life of the SFT-C. This change of philosophy is grounded in three facts. First, since the cause of the potentiometer failures has not been definitively established, it seems prudent to install several instrument types in an attempt to minimize the likelihood of further mass failures. Second, installation of several instrument types would facilitate an evaluation of the relative performance of the selected instruments. Third, judicious choice of alternative transducers would not lead to degradation in the quality of acquired data and may even improve the quality.

These three considerations led to selection of four transducers to replace the 48 GBE- and GCE-series units where all failures have occurred to date (see Fig. 1). Each group of three extensometers received one type of transducer. Bourns Model 5184 rectilinear potentiometers were reinstalled in GBE24x, GBE25x, and GBE26x. Vernitron Model 113 rectilinear potentiometers were installed in GCE24x, GCE25x, and GCE26x. Schaevitz Model 250HCD linear variable differential transformers (LVDT/DCDT) were installed in GBE21x, GBE22x, and GBE23x. Kaman Model KD-2310-6U electromagnetic proximeters were installed in GCE21x, GCE22x, and GCE23x. Table 5 summarizes the characteristics of the selected transducers. Each of the three alternates compares favorably in several ways with the original Bourns potentiometers (see Fig. 5).

The Vernitron potentiometer has more favorable specifications for linearity, actuation force, and operating temperature range, and it meets all other specifications (see Fig. 6). Installation of these units required shortening of the three head assembly stand-off legs by about 25 mm to accommodate the shorter case length.

The Schaevitz DCDT possesses more favorable resolution, hysteresis, and linearity characteristics, has a broader operating temperature range, and requires no force to actuate the core (see Fig. 7). These advantages are achieved at the cost of range. Prior to actual field experience, we would

Table 5. Summary of replacement transducer characteristics.

Parameter	Bourns Model 5184	Vernitron Model 113	Schaevitz Model 250 HCD	Kaman Model KD-2310-6U
Case diameter (mm)	12.7	12.7	19.0	19.0
Case length (mm)	90	60	104	25
Power supply (Vdc)	10	10	±15	±12
Range (mm)	25	25	±6	±3
Resolution (μm)	2.5	2.5	0.6	0.6
Linearity (% full scale)	±1.0	±0.1	±0.25	±0.50
Hysteresis (% full scale)	0.1	0.1	none	none
Stability (% full scale)	N/A	N/A	0.125	±0.01/mo
Temperature coefficient (μm/°C)	N/A	N/A	<4.8	<2.4
Actuation force (g)	570	230	0	0
Temperature range (°C)	-30 to 80	-55 to 125	-55 to 95	0 to 55

have questioned the ±6 mm range. Based on test results to date, it is acceptable. The unit has a potential instability related to drift in electronic components. *In situ* calibrations will document any instabilities. The temperature coefficient of the transducer is not expected to produce errors in excess of about 60 μm during the life of the SFT-C. The larger case diameter of the DCDT required boring out the four mounting plate holes to 19 mm and constructing larger clamping fixtures. A ±15 Vdc power supply was also required.

The Kaman Model KD-2310-6U proximeters also possess better resolution, hysteresis, and linearity specifications in comparison with the original Bourns potentiometers (see Fig. 8). Since these units are not mechanically coupled to the extensometer rod, problems such as side loading due to shaft misalignment are eliminated. Once again, the cost of these improvements is decreased range. Instabilities in electronic components are likely with these units and must be monitored with *in situ* calibrations. The temperature coefficient of the proximeters should not introduce errors in excess of about

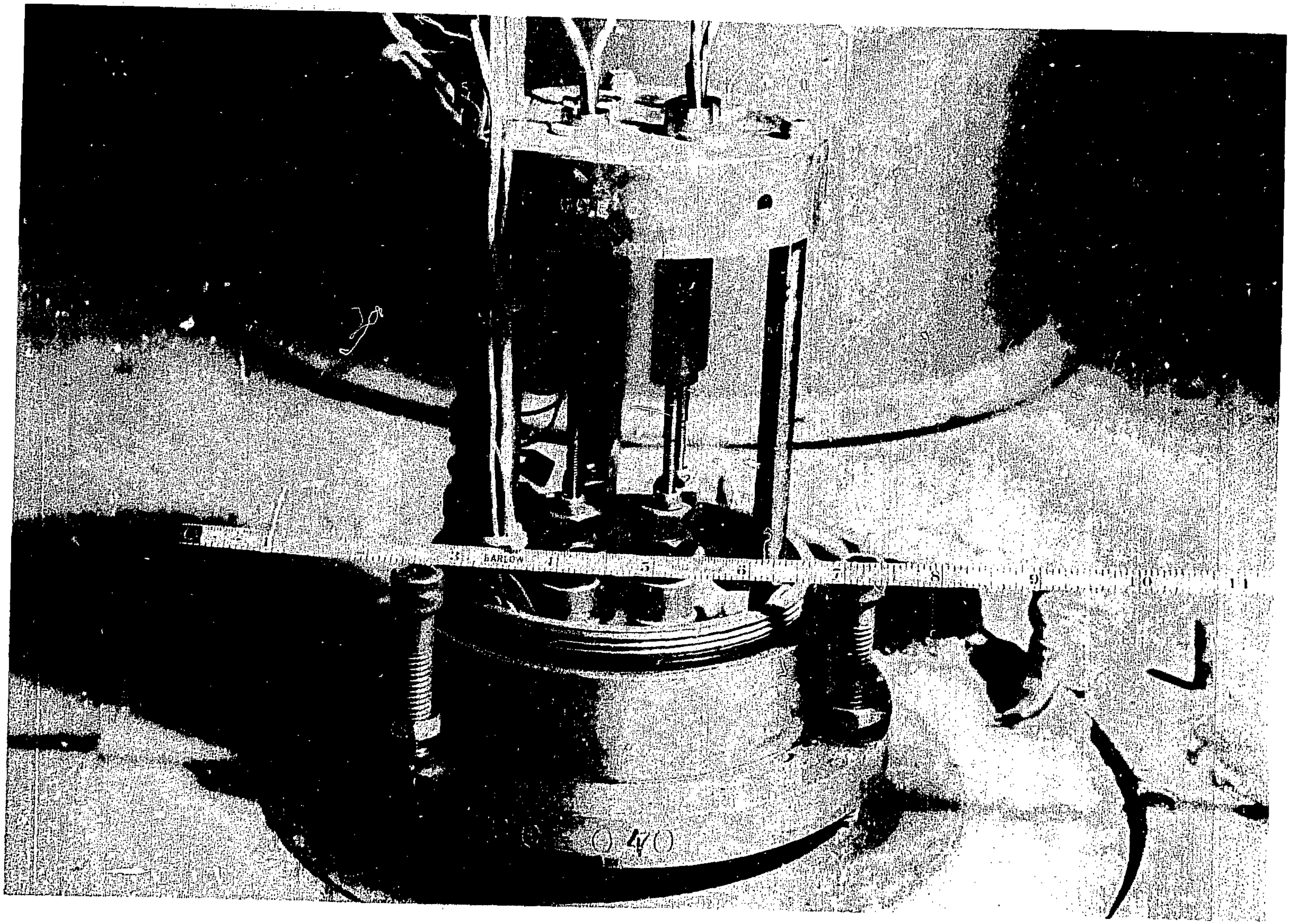

FIG. 5. GCE extensometer with Bourns potentiometers and screw couplings.

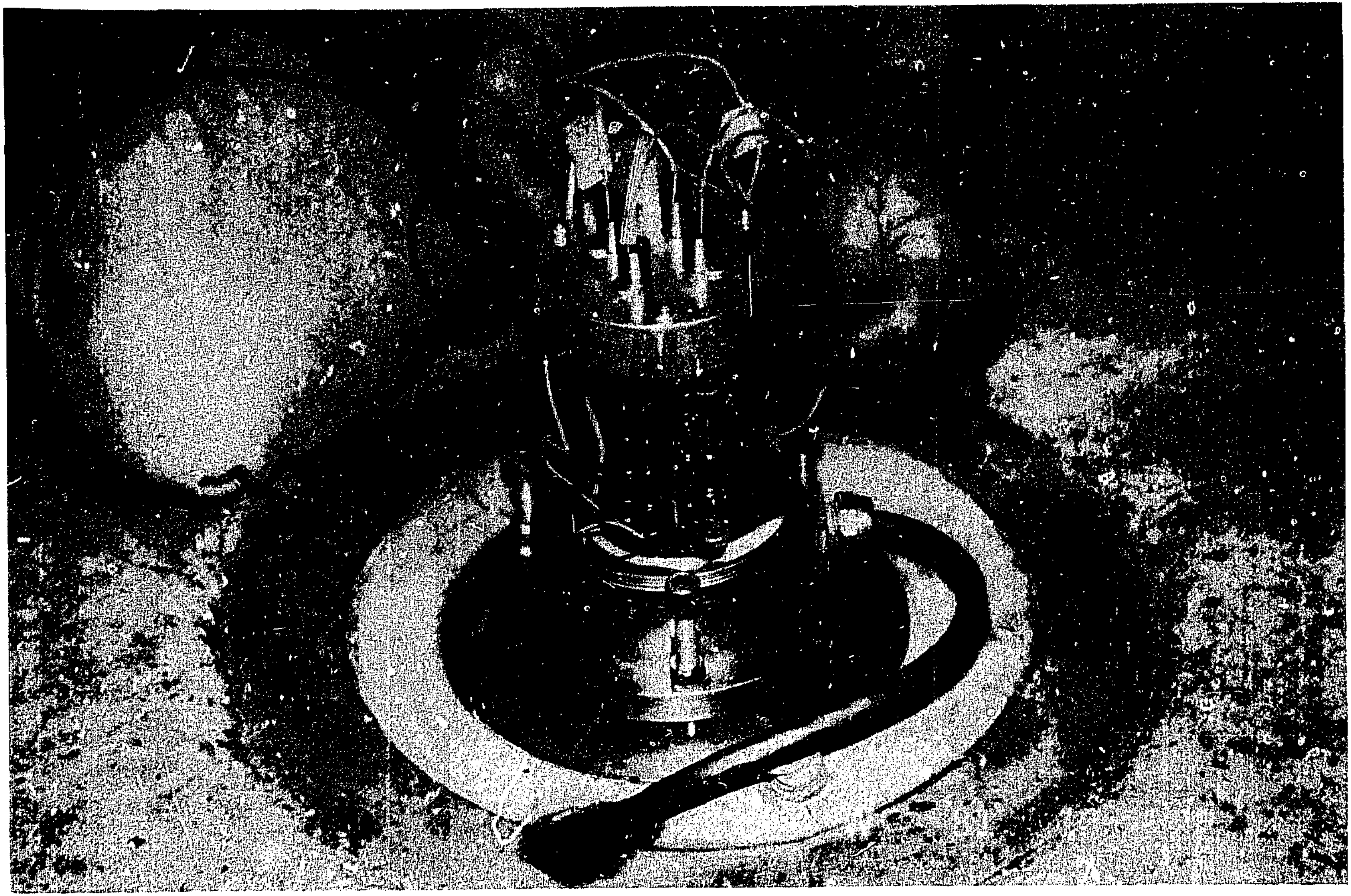

FIG. 6. G-series extensometer showing spring-loaded couplings used with Vernitron and replacement Bourns potentiometers.

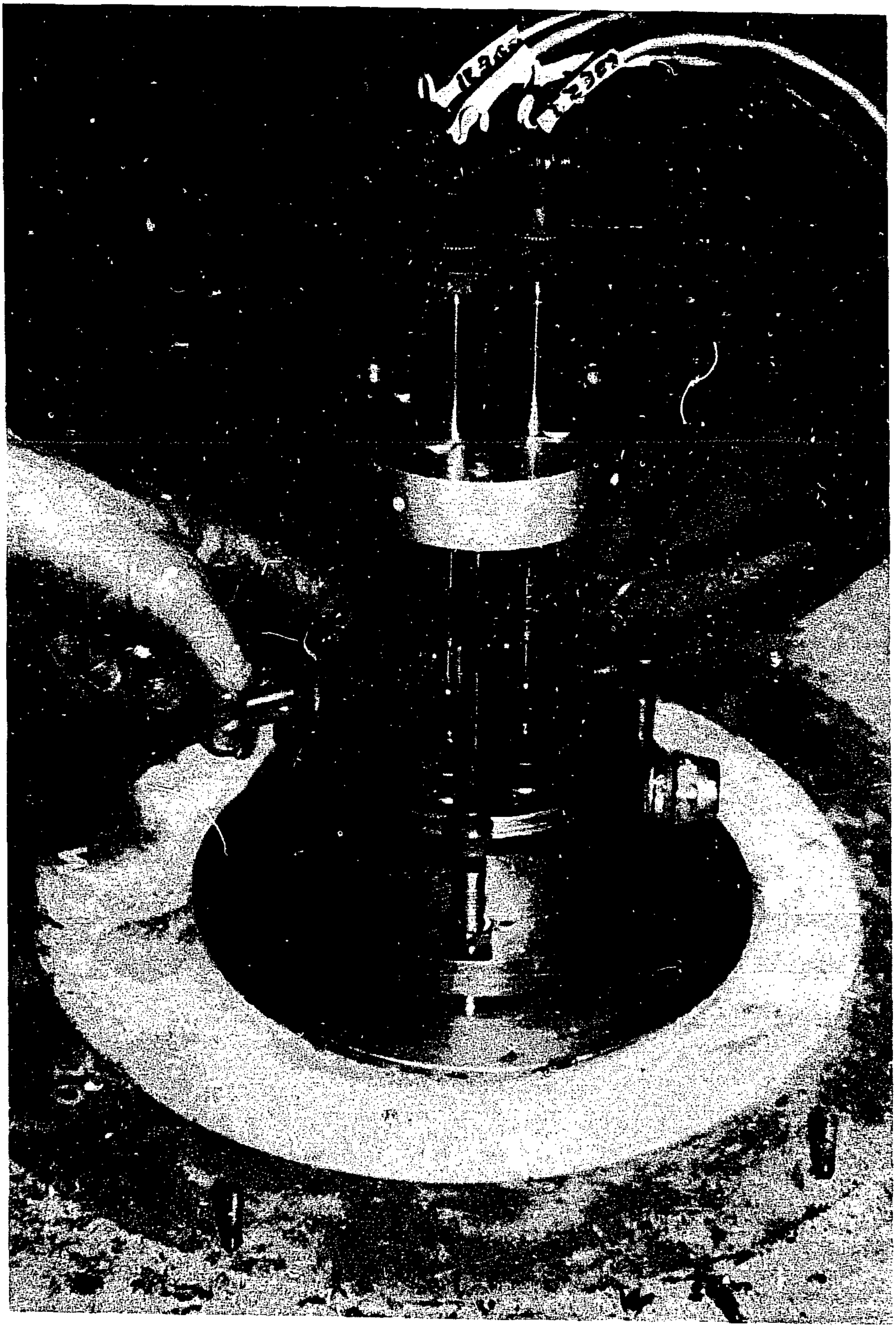

FIG. 7. GBE extensometer with Schaevitz LVDT's.

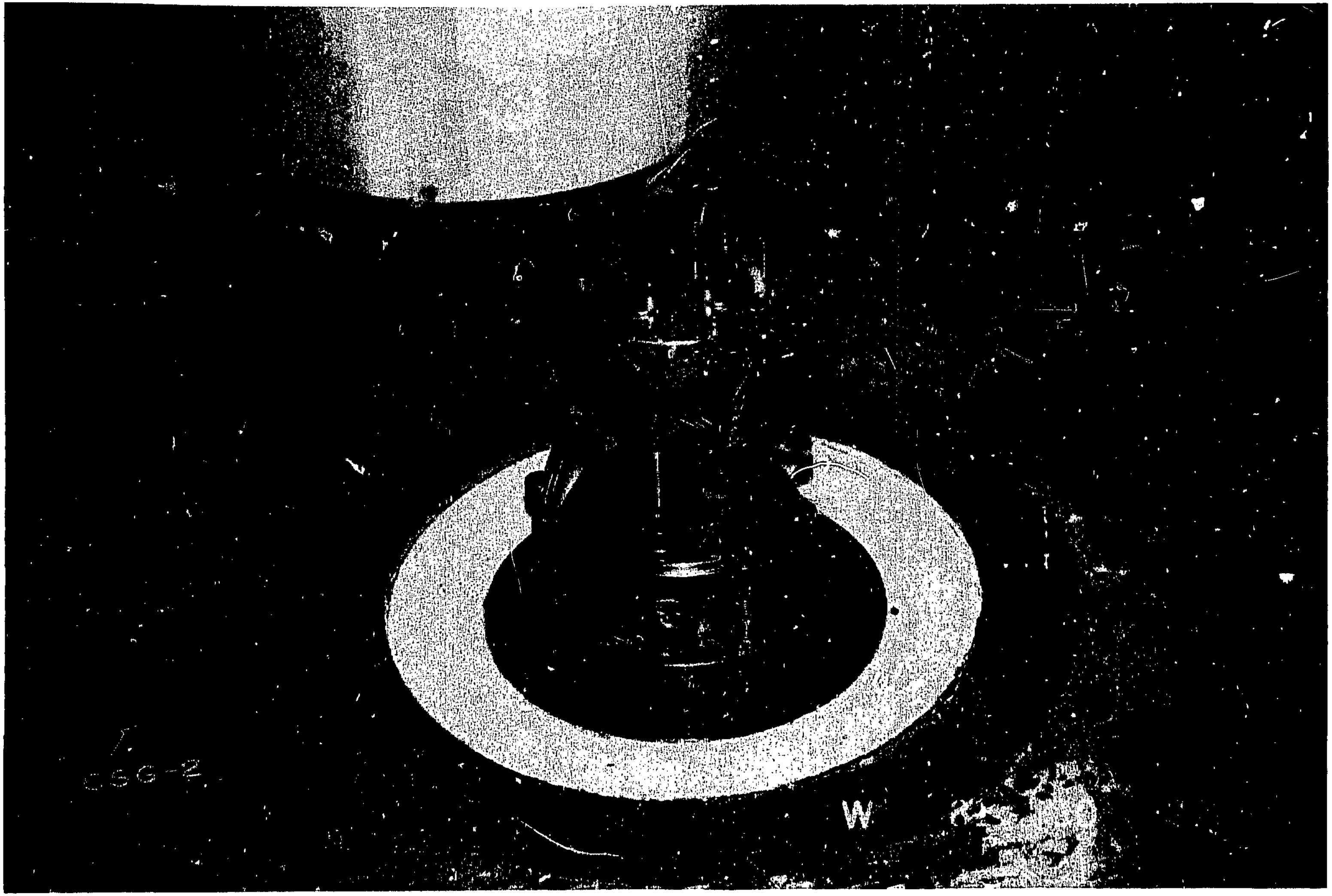

FIG. 8. GCE extensometer with Kaman proximeters.

30 μm during the life of the SFT-C. A narrower range of operating temperatures is specified for these units. No direct modifications to the head assembly were required to implement the proximeters. The basic unit was installed in an LLNL holder which coupled with the standard head assembly. A cylindrical shield was fabricated to permit use of these devices in close proximity of each other. These units required a ±12 Vdc power supply and associated signal conditioning.

We had observed in previous installations that some nonconcentricity existed between potentiometer shafts and the rods to which they were coupled. This condition introduces side loading which causes binding of the shaft and body of the potentiometers. This phenomenon may be responsible for some of the "stick-slip" type motion observed in the rod extensometers. During replacement operations, a modification was introduced to circumvent this problem. All screw couplings of potentiometer and DCDT shafts to rods were replaced by spring loading the shaft against a flat smooth stainless steel fitting attached to the rod (see Figs. 5-7). A stainless steel sphere screwed onto the shaft provides essentially a point contact against the stainless steel fitting attached to the rod. This modification was implemented on both potentiometer types and the DCDT. The proximeter is a noncontacting device which utilizes a 19-mm-diam by 6.4-mm-thick aluminum target attached to the rod. These modifications are expected to enhance the quality of the acquired data.

Another modification that we implemented was to subject each of the head assemblies associated with the Bourns, Vernitron, Schaevitz, and Kaman transducers to three different environments. The three selected environments were (1) normal with the cover on the head assembly, (2) flushed with dry nitrogen, and (3) ventilated of potentially harmful vapors with a slight vacuum. Should further transducer failures occur, the different environments should provide new data on the potential causes of failure.

As an added precaution, all Vishay precision resistors were replaced with hermetically sealed units. This change was implemented in response to the two observed failures.

All refurbished rod extensometers were calibrated _in situ_ in accordance with established procedures.[4] Prior to _in situ_ calibration, all transducers were laboratory calibrated. Because of the shorter range of the Schaevitz and Kaman transducers, these units were calibrated in 0.5-mm steps over a range of 2.5 mm rather than in 1.0-mm steps over a range of 5.0 mm.

VIBRATING-WIRE STRESSMETER FAILURES

Incorporated in the approximately 850 channels of data being recorded on the SFT-C are 18 vibrating-wire stressmeters (VWSM) produced by IRAD Gage, a division of Creare Products, Inc., Lebanon, New Hampshire. Since their installation in March 1980, 13 of the 18 gauges have failed. The mechanism of failure has been identified as internal rusting, especially of the wire itself. IRAD has redesigned the gauge, providing a welded hermetic seal in place of the "O" ring seal previously used. Nine gauges of the new design were reinstalled in place of failed units on 16 to 17 June 1981. To date, all of these new units appear to be functioning normally.

INSTRUMENT DESCRIPTION

The complete system consists of the 18 gauges, 2 switch modules, and 1 data logging unit, connected as shown in Fig. 9. The gauge itself is quite simple and rugged as shown in exploded view in Fig. 10. This figure shows an early version of the gauge. More recent gauges have two epoxy plugs inserted from opposite ends of the gauge after the vibrating wire is in place. One plug contains the core magnet assembly and cable exit; the other plug is solid epoxy.

The body of the gauge consists of a hollow steel cylinder which, in use, is secured in a 1-1/2-in.-diam borehole by a substantial preload established by a sliding wedge and platen assembly. Stress changes in the surrounding rock cause small changes in the diameter of the cylinder which are measured as changes in the natural frequency of vibration of a steel wire stretched across the diameter to the cylinder walls. By calibration, changes in the wire period (i.e., the time for one cycle of vibration) have been related to the magnitude of stress change for a range of rock types.

The coil/magnet assembly generates an electrical signal analogous to the wire motion. This signal is amplified in the data logger and is used to control a circuit counting the number of pulses from a 100 kHz clock occurring over a period of 100 oscillations of the wire. Thus, if the period of the wire is 200 μs, the reading from the data logger is 2000.

The wire is set into vibration by a 10-V swept-frequency signal applied to the coil by the data logger just prior to each measurement. If the data

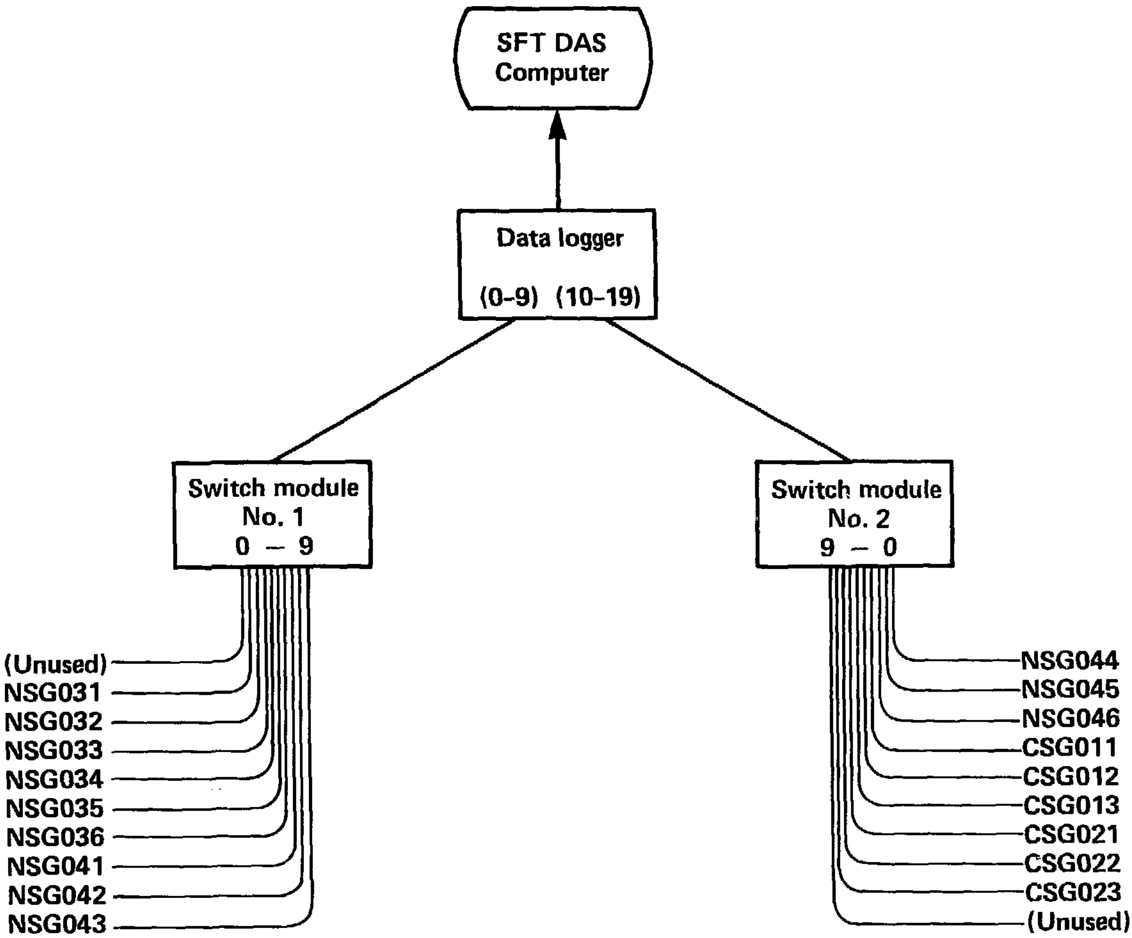

FIG. 9. SFT VWSM system as installed March 1980.

logger's error detection circuitry determines that the reading is unreliable, the reading is set to 0000.

The normal range of readings is from R_o to 4000 where R_o is the no-load reading of the gauge before installation (see Tables 6 and 8). For the gauges installed to date, R_o has been in the range 1815 to 2268 ($\bar{x}$ = 2049, σ_x = 124).

Two versions of the gauge were available at the time of the initial procurement: the standard gauge and a high temperature version, VBS-1HT. The high temperature version was identical in construction to the standard gauge; however, it used higher temperature materials for potting compounds, O-ring seals, and cable insulation, and its body was heat treated to higher

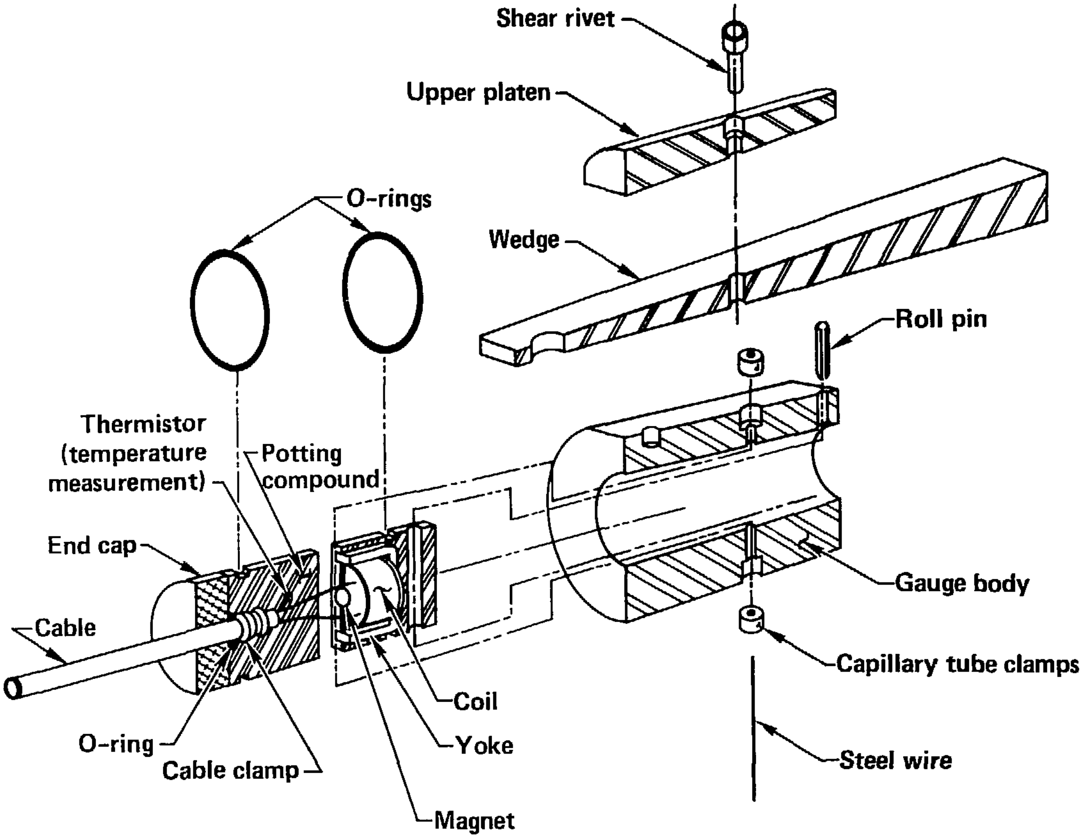

FIG. 10. Vibrating-wire stressmeter (section view through body).

temperature before assembly. Lawrence Livermore National Laboratory requested a nickel plated version of the VBS-1HT and has renamed it the "UCL^3" gauge.

A SUMMARY HISTORY AND IDENTIFICATION OF THE PROBLEM

The initial installation of the gauges was accomplished 18 to 20 March 1980. The system was as shown in Fig. 9 except that the computer link was unavailable and output was to a "Silent 700" teletype (TTY) terminal, giving readouts every four hours. The locations and initial readings of these gauges are given in Table 6. Figure 11 shows the teletype output for the first minutes of recorded data. Here data is sampled once per minute. Recording began on 1 April 1980 (day 92) at 14:29 Pacific standard time (PST). On 27 April (day 118), the system clock was switched to Pacific daylight savings time (PDT).

Table 6. Gauge data for March 1980 installation.

Gauge name	Serial No.	IRAD channel	Depth[a] (m)	Orientation	Zero	Tool set	Tool removed	Δ (%)
NSG031	Q9	1	2.794(N)[b]	60°CW	2122	2322	2300	11
NSG032	Q13	2	3.023(N)	Vert	1837	2058	2042	7
NSG033	Q18	3	3.302(N)	60°CCW	1918	2122	2122	0
NSG034	Q17	4	0.597(C)[c]	60°CW	2186	2416	2401	7
NSG035	Q22	5	0.711(C)	Vert	2177	2397	2372	11
NSG036	Q26	6	0.825(C)	60°CCW	2028	2230	2222	4
NSG041	O11	7	2.896(N)	60°CW	2181	2429	2421	3
NSG042	O20	8	3.289(N)	Vert	2200	2405	2391	7
NSG043	O3	9	3.404(N)	60°CCW	1878	2090	2089	0
NSG044	O12	10	0.457(C)	60°CW	2072	2275	2240	17
NSG045	O23	11	0.572(C)	Vert	2121	2349	2343	3
NSG046	O24	12	0.686(C)	60°CCW	2200	2404	2394	5
CSG011	O7	13	3.505	60°CW	2049	2389	2384	1
CSG012	Q15	14	3.658	⊥ Rail	2018	2233	2205	13
CSG013	O5	15	3.810	60°CCW	2016	2232	2227	2
CSG021	Q1	16	3.353	60°CW	2188	2397	2398	0
CSG022	Q27	17	3.658	⊥ Rail	1839	2053	2035	8
CSG023	Q4	18	3.810	60°CCW	1924	2129	2124	2

[a] Hole NSG03 is 5.842 m long. Hole NSG04 is 5.702 m long.
[b] (N) is depth measured from north drift.
[c] (C) is depth measured from center drift.

At 13:18 PDT on 14 August 1980 (day 227), the system was taken down so the data logger could be used to test and debug the newly constructed computer interface unit. At this time it was noticed that IRAD channel 16 had been reading 0000 since 20:16 PDT on 7 August and channel 15 had been reading 0000 since 00:16 PDT on 13 August. A period of sporadic zeros preceded the failures and had appeared on IRAD channels 17 and 18 at the end of the record, suggesting impending failure of those instruments. The signal leads were tested for continuity through the coil and leakage to ground, and were found to be normal.

```
0092[a]1429[b]
00 0000 2281 2033 2117 2372 2354 2214 2412 2388 2074
10 2231 2329 2369 2376 2168 2221 2379 2026 2116 0000
20
0092 1430
00 0000 2281 2033 2117 2372 2354 2213 2413 2388 2074
10 2231 2330 2370 2376 2167 2222 2379 2026 2116 0000
20
0092 1431
00 0000 2281 2033 2117 2372 2354 2213 2413 2387 2074
10 2232 2329 2370 2376 2168 2222 2379 2026 2116 0000
20
0092 1433
00 0000 2280 2033 2117 2372 2354 2214 2412 2388 2075
10 2232 2330 2369 2376 2168 2222 2380 2026 2116 0000
20
0092 1434
00 0000 2281 2033 2117 2372 2354 2213 2412 2387 2073
10 2231 2329 2369 2376 2167 2221 2380 2026 2116 0000
20
0092 1435
00 0000 2280 2033 2116 2372 2354 2213 2413 2388 2075
10 2232 2330 2369 2376 2168 2222 2380 2026 2116 0000
20
0092 1436
00 0000 2281 2033 2116 2372 2354 2213 2413 2388 2074
10 2231 2330 2370 2377 2168 2221 2380 2026 2116 0000
20
0092 1437
00 0000 2280 2033 2117 2372 2354 2214 2413 2388 2074
10 2232 2330 2370 2376 2168 2221 2380 2025 2116 0000
20
0092 1439
00 0000 2281 2033 2117 2372 2354 2214 2412 2387 2074
10 2231 2330 2369 2376 2167 2222 2379 2025 2117 0000
20
0092 1440
00 0000 2281 2033 2117 2372 2354 2213 2413 2388 2074
10 2231 2329 2370 2376 2167 2222 2379 2026 2115 0000
20
0092 1441
00 0000 2281 2032 2117 2372 2355 2214 2413 2388 2074
10 2231 2330 2369 2376 2167 2221 2379 2025 2116 0000
20
0092 1442
00 0000 2280 2033 2117 2372 2354 2213 2412 2388 2074
10 2231 2330 2369 2377 2168 2222 2380 2025 2116 0000
20
0092 1443
00 0000 2280 2033 2117 2372 2354 2214 2413 2388 2074
10 2232 2329 2369 2376 2168 2222 2380 2026 2116 0000
20
```

[a]Day of the year (0092 = 01 April 80).

[b]Time of day (PDT).

FIG. 11. Example of VWSM teletype record.

By 22 August, the TTY data had been punched on cards, and codes had been written to convert it to a form readable by a plot program. Figure 12 shows the plottable form of the data for the last few days before the system take-down. Figure 13 shows the plotted data in units of stress for the four suspect gauges and two "normal" gauges. Note that the normal curves are smooth and approach a constant stress value of 0.4 MPa, while the suspect units show stress and erratic behavior increasing with time until they failed. The TTY readout system was re-established at 14:11 PDT on 29 August (day 242). At this time all four suspect channels (15, 16, 17, and 18) were reading 0000.

When the manufacturer was contacted, they recommended that an attempt be made to read the gauges with an MB-6 readout device. The MB-6 allows one t tune the excitation signal to the gauge being read and provides test points for observing the signals on an oscilloscope. The instrument was shipped to LLNL by IRAD as a loan, and the measurements were made on 23 September, with the following results.

A reading of 2420 was obtained on channel 18. Readings could not be produced on channels 15, 16, or 17; although by careful tuning, it was possible to get the wires to vibrate on channels 15 and 17. This, along with the oscilloscope pictures, led us to conclude that the gauge wires had suffered a decrease in Q (i.e., increased mechanical damping) that caused the wire vibrations to die out too quickly for the data logger to obtain a reading. IRAD was sent copies of the oscilloscope pictures,[6] and they concurred in the LLNL conclusion.

On 30 September 1980, a spare gauge (Serial No. 02) was suspended in hole CSG02 without clamping, as an environmental test. The subsequent response of this gauge is given in Fig. 14. Notwithstanding the fact that the gauge has zero imposed stress, it shows an initial drop in reading followed by a gradual but pronounced increase until failure on 14 November 1980 (day 319).

On 26 November, the computer link was established between the IRAD data logger and the DAS, so TTY output was ended.

Evaluation of Failures

Since all available data indicated that the failure was in the gauges themselves and not somewhere in the cabling or data logging system, we decided to attempt to remove the gauges in the two vertical holes. Additional failed

JULIAN DAY	IRAD CHANNEL NUMBER Ø	1	2	3	4	5	6	7	8	9	1Ø	11	12	13	14	15	16	17	18	19
44463.136	.Ø	2291	2Ø44	2118	24Ø2	241Ø	2215	2419	238Ø	2Ø66	2216	2359	236Ø	2494	2226	243Ø	.Ø	2244	2487	.Ø
44463.3Ø3	.Ø	2291	2Ø44	2118	24Ø1	24Ø9	2216	2419	238Ø	2Ø66	2216	2359	236Ø	2495	2226	2433	.Ø	2219	2487	.Ø
44463.469	.Ø	229Ø	2Ø44	2118	24Ø2	241Ø	2216	2418	2379	2Ø66	2216	2359	236Ø	2495	2226	.Ø	.Ø	2214	2486	.Ø
44463.636	.Ø	2291	2Ø44	2118	24Ø1	241Ø	2216	2419	2379	2Ø66	2216	2358	236Ø	2495	2226	2433	.Ø	2216	2488	.Ø
44463.8Ø3	.Ø	2291	2Ø44	2119	24Ø2	241Ø	2215	2419	2379	2Ø66	2216	2358	236Ø	2495	2226	2435	.Ø	2221	2489	.Ø
44463.969	.Ø	229Ø	2Ø45	2118	24Ø1	241Ø	2216	2419	2379	2Ø66	2217	2357	236Ø	2495	2226	2434	.Ø	2225	2491	.Ø
44464.136	.Ø	2291	2Ø44	2118	24Ø2	241Ø	2216	2419	238Ø	2Ø66	2216	2356	2361	2496	2226	2434	.Ø	2225	2489	.Ø
44464.3Ø3	.Ø	2291	2Ø44	2118	24Ø2	241Ø	2216	2419	238Ø	2Ø66	2216	2358	2361	2495	2226	.Ø	.Ø	2228	2486	.Ø
44464.469	.Ø	2291	2Ø45	2119	24Ø1	241Ø	2216	242Ø	238Ø	2Ø66	2216	2359	236Ø	2495	2226	2439	.Ø	2223	2485	.Ø
44464.636	.Ø	2291	2Ø45	2118	24Ø2	241Ø	2216	2418	2379	2Ø65	2216	2358	2361	2496	2226	2437	.Ø	2223	247Ø	.Ø
44464.8Ø3	.Ø	2291	2Ø44	2118	24Ø2	241Ø	2216	2418	2379	2Ø66	2217	2358	2361	2495	2226	2436	.Ø	.Ø	.Ø	.Ø
44464.969	.Ø	2291	2Ø45	2119	24Ø1	241Ø	2216	2418	238Ø	2Ø66	2216	2356	2361	2496	2226	2437	.Ø	2229	2489	.Ø
44465.136	.Ø	2291	2Ø45	2118	24Ø2	241Ø	2216	2418	238Ø	2Ø66	2217	2357	2361	2495	2226	2441	.Ø	223Ø	2468	.Ø
44465.3Ø3	.Ø	2291	2Ø44	2118	24Ø2	241Ø	2215	2419	2379	2Ø66	2216	2355	2361	2495	2226	2439	.Ø	2231	2494	.Ø
44465.469	.Ø	2292	2Ø45	2118	24Ø2	241Ø	2216	2418	2379	2Ø66	2217	2354	2361	2495	2227	2441	.Ø	2231	2479	.Ø
44465.636	.Ø	2292	2Ø45	2118	24Ø2	241Ø	2215	2418	238Ø	2Ø67	2216	2354	2361	2495	2226	2441	.Ø	2235	24Ø6	.Ø
44465.8Ø3	.Ø	2291	2Ø45	2118	24Ø2	241Ø	2216	2419	238Ø	2Ø66	2216	2354	2362	2495	2227	.Ø	.Ø	2235	24Ø5	.Ø
44465.969	.Ø	2291	2Ø45	2118	24Ø3	2411	2216	2419	2379	2Ø66	2217	2354	2361	2495	2226	.Ø	.Ø	224Ø	2418	.Ø
44466.136	.Ø	2292	2Ø44	2119	24Ø2	2411	2216	2419	2379	2Ø66	2217	2354	2362	2496	2226	.Ø	.Ø	2236	2438	.Ø
44466.3Ø3	.Ø	2292	2Ø45	2118	24Ø3	2411	2215	2418	238Ø	2Ø66	2216	2354	2361	2495	2226	.Ø	.Ø	2239	2448	.Ø
44466.346	.Ø	2292	2Ø45	2119	24Ø3	2411	2216	2419	238Ø	2Ø66	2216	2354	2362	2495	2226	.Ø	.Ø	2244	2453	.Ø

FIG. 12. Reformatted VWSM data.

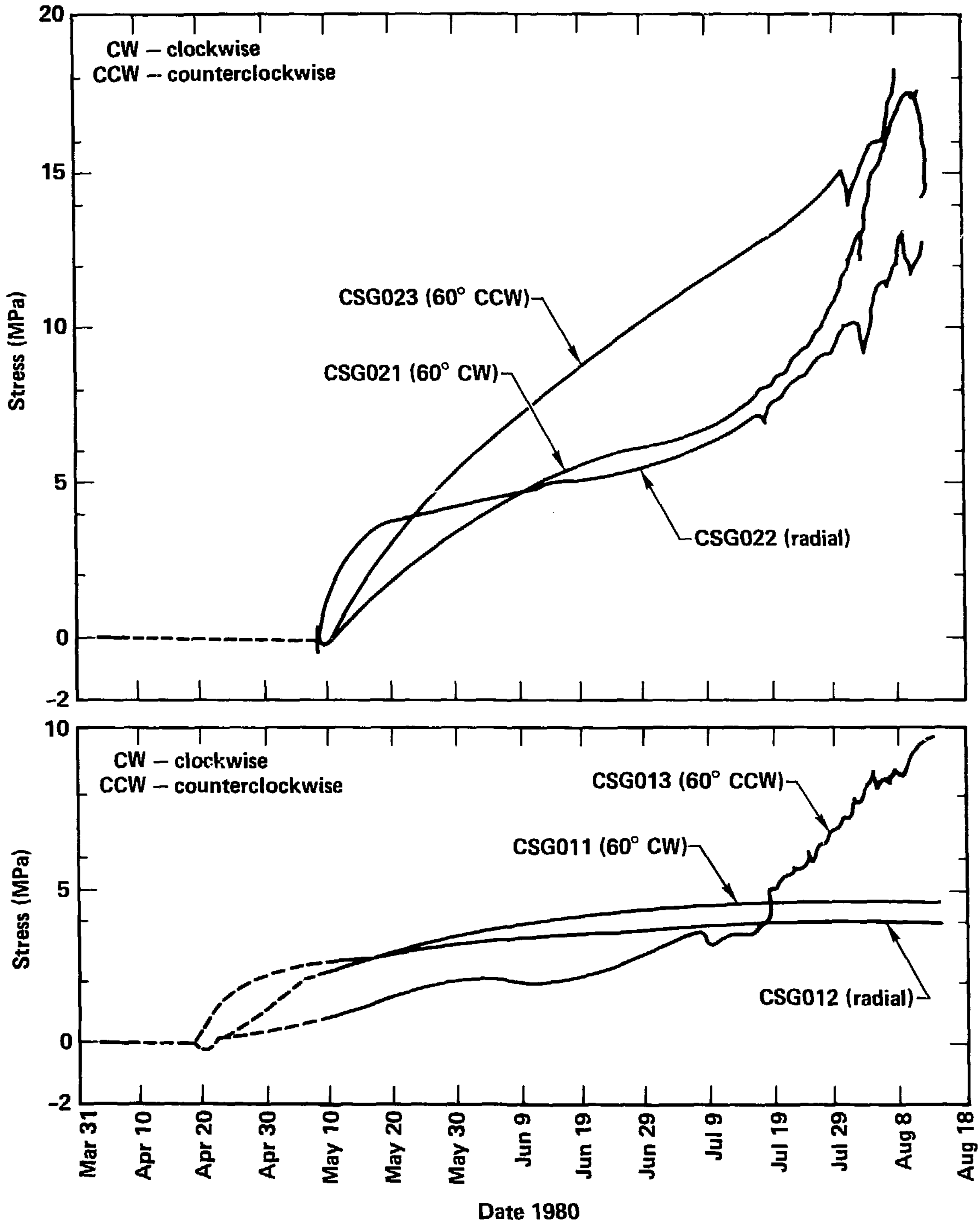

FIG. 13. Plots of data from selected gauges.

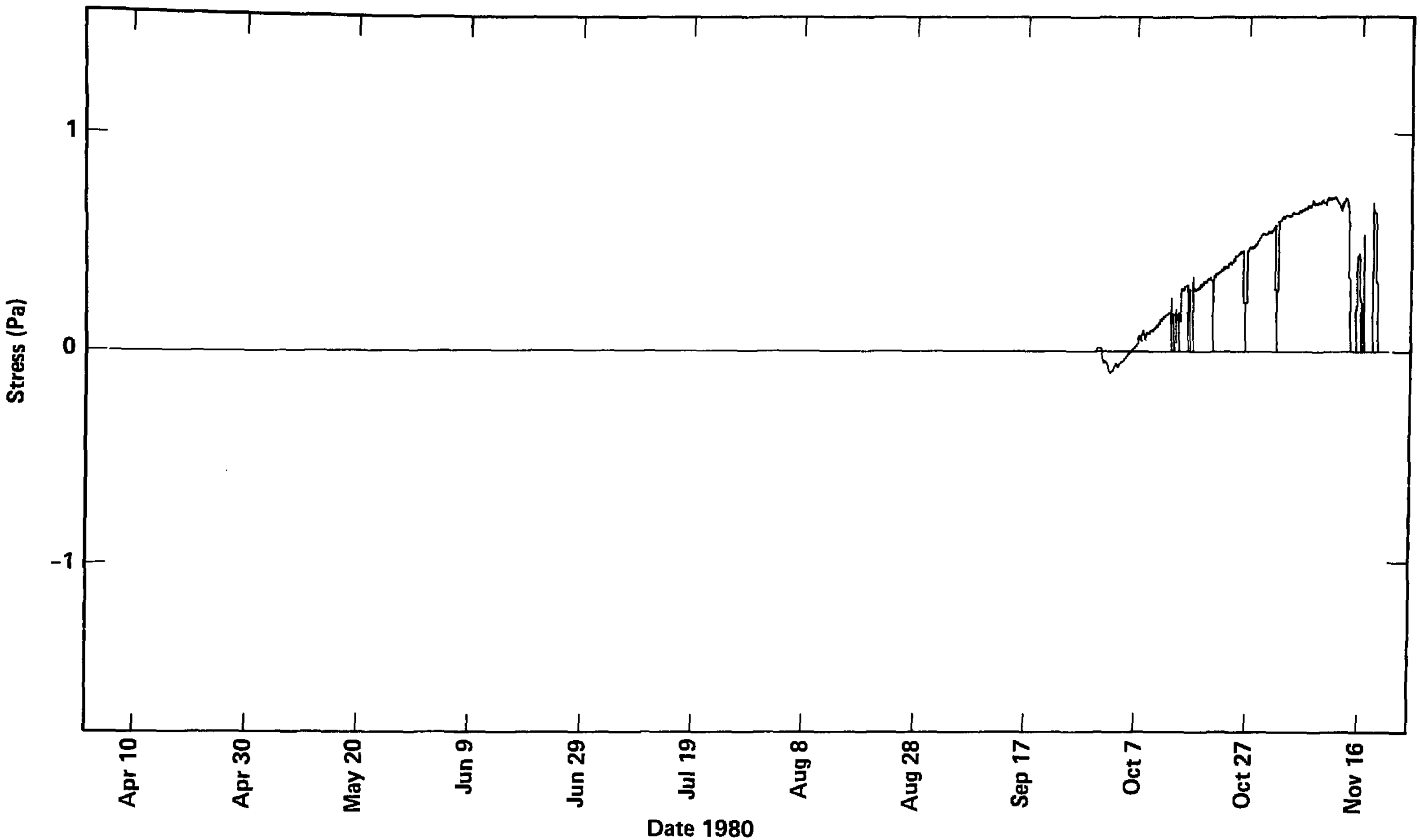

FIG. 14. Data from "free" gauge in CSG02.

gauges in NSG04 could not be removed without disturbing the functional gauges. Removal was complicated by the fact that a closed-cell polystyrene foam had been cast in place around the gauges to minimize their exposure to groundwater. Mock-up tests in Livermore showed that the foam could be removed by sand blasting without damage to the gauges or cables. There was an unsuccessful attempt at removal on 10 December 1980. On 19 December 1980 these six gauges were removed and sent to Lawrence Livermore National Laboratory, Livermore, California. Radiation background readings were made in the two holes. The results are shown in Table 7. These readings are far below any level which might affect the gauges significantly, and the difference in readings is apparently due to differing distances of the two holes from the nearest spent fuel canister.

When the gauges arrived, the seal plug of one gauge was removed to allow inspection of the interior. Figure 15 shows the results. The wire itself is coated with red crystals which under X-ray analysis appear to be goethite, an iron oxide. On 2 February 1981, the gauges were taken to the IRAD plant in Lebanon, New Hampshire, where two of the gauges were sawn apart. The cut was made near enough to the sensing wire to allow close inspection of it but not so close to disturb the wire or coatings it may have acquired. The wires of both of these gauges also were rusted. With pressurized air a test was made of the O-ring seals in the two ends of each of the sawn apart gauges, with the result that one gauge showed a small air leak through the magnetic core region of one end plug. The other gauge showed a small air leak between the O-ring

Table 7. Radiation reading in CSG01 and CSG02, 19 December 1980.

Depth below floor (ft)	Radiation readings CSG01 (mr/h)	CSG02 (mr/h)
0	0.02	0.02
4	0.50	2.0
5	2.0	3.0
7	4.0	10.0
10	4.0	14.0
13	3.0	15.0

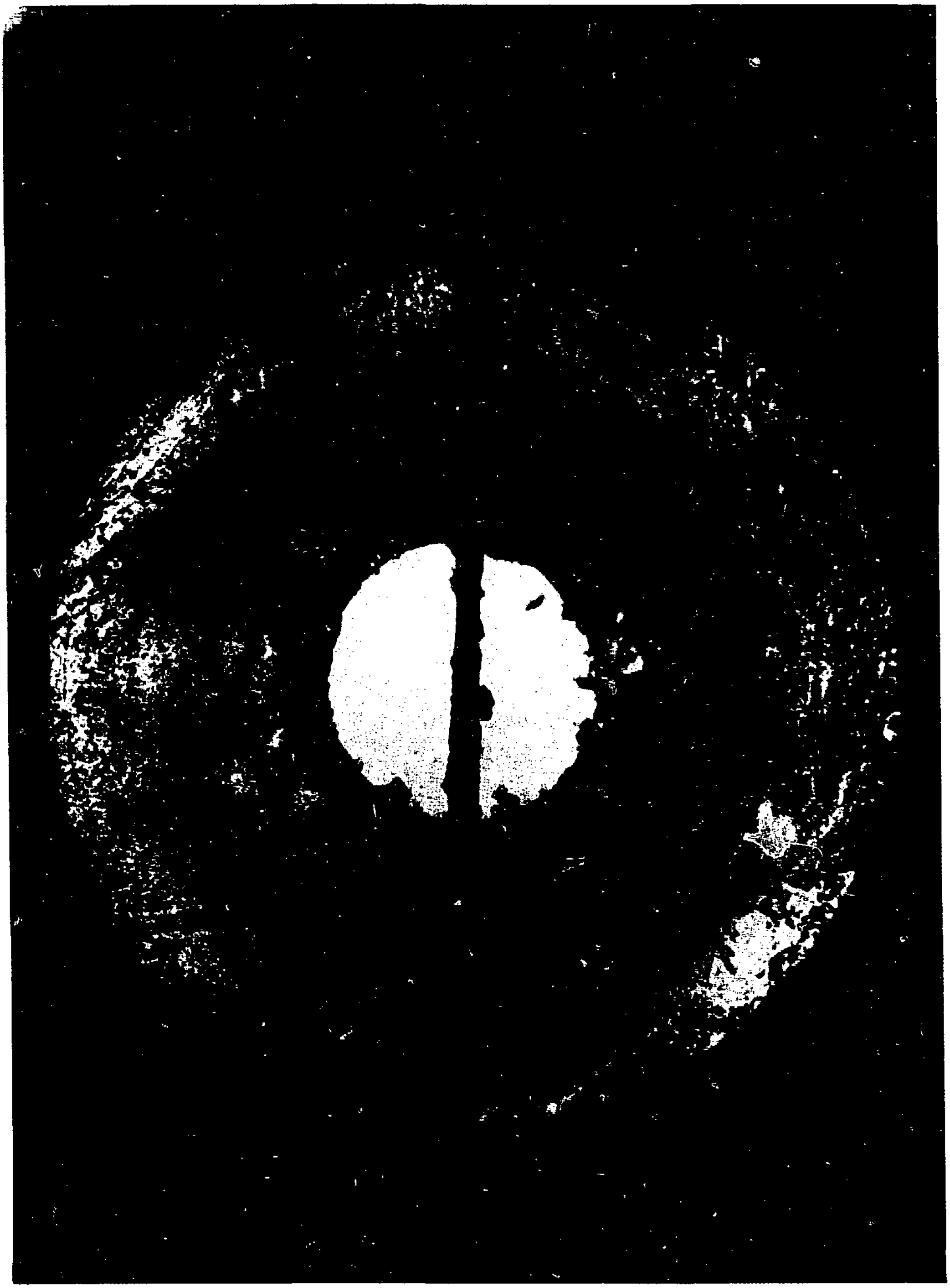

FIG. 15. Interior of failed VWSM.

and the epoxy plug opposite the magnetic core plug. Inspection of the suspect plug showed a small amount of mold flashing at the bottom of the O-ring groove at the apparent site of the leak. Normally, these mold marks are removed with a fine file before assembly, but this unit apparently got through IRAD inspection by mistake.

Our present understanding of the problem is as follows:

1. Moisture enters at least some gauges through faulty O-ring seals or faulty potting of the magnet core assembly.
2. Since the gauges are not flushed with dry Nitrogen or other gas at assembly, the possibility remains that sufficient moisture in the form of humid air is introduced into the gauge during assembly which ultimately perturbs the gauge reading by wire rusting.
3. The LLNL specification of nickel plating inside the gauge body may have exacerbated the problem by removing a rustable surface within the gauge which otherwise might act as a "getter" for whatever water was present. This would probably only be significant for item 2 above where a limited amount of moisture is available.

Remedial Actions

Under independent funding, IRAD subsequently designed and tested a hermetically sealed version of the gauge. In the new version, sealing is accomplished by thin stainless steel cups welded to the gauge body around the perimeter of the hole at the ends of the gauge (see Fig. 16). Since the welding is done by electron beam, the interior of the gauge is a hard vacuum, eliminating any moisture entry at assembly.

Following a number of production problems, nine of the new gauges were installed at the SFT-C 16 to 17 June 1981. The location and orientation of each gauge was precisely selected to avoid rough spots, fractures, and residual foam on the wall contact areas. A borescope was used to select the appropriate locations. Locations and initial readings of the gauges are given in Table 8. The change in reading in the first 24 hours is due to the gauges coming into thermal equilibrium with the rock. To date all of these gauges appear to be functioning normally.

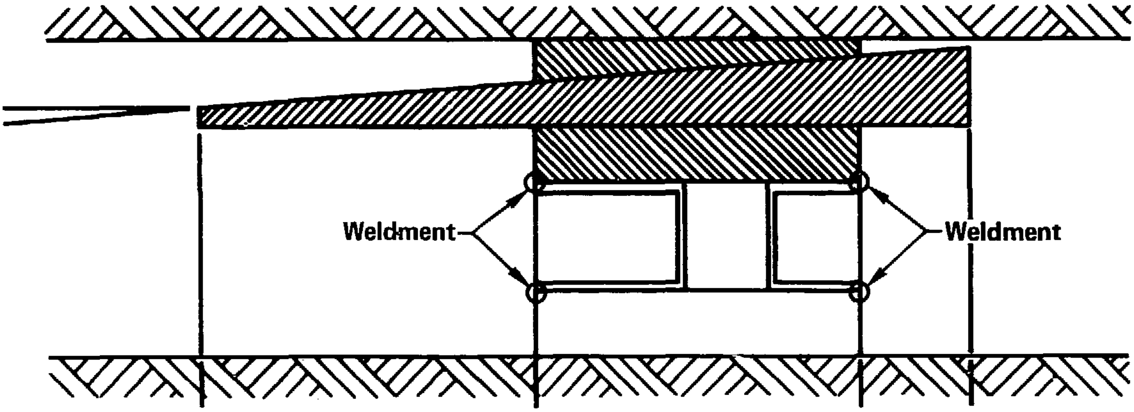

FIG. 16. Use of thin stainless cups in the new gauge.

Table 8. Gauge data for June 1981 installation.

Gauge name	Serial No.	IRAD channel	Depth[a] (m)	Orientation	Gauge reading Zero	Tool set	Tool removed	Δ (%)	Next day
NSG241	RD135	7	2.65(N)[b]	60° CW	2061	2500	2480	5	2465
NSG242	9	8	2.80(N)	Vert	2268	2500	2514	-6	2496
NSG243	RD116	9	2.95(N)	60° CCW	2041	2246	2208	19	2200
CSG211	RD125	13	3.50	60° CCW	1947	2186	2146	17	2154
CSG212	RD122	14	3.65	⊥ Rail	2037	2275	2245	13	2299
CSG213	RD130	15	3.80	60° CW	1998	2222	2163	26	2188
CSG221	RD132	16	3.45	60° CCW	2065	2307	2343	-15	2395
CSG222	RD133	17	3.60	⊥ Rail	2085	2331	2312	8	2368
CSG223	RD124	18	3.75	60° CW	1815	2050	2029	9	2059

[a] Hole NSG04 (containing gauges NSG241, 242, and 243) is 5.702 m long.
[b] (N) means depth measured from north drift.

SUMMARY AND CONCLUSIONS

Less than six months after spent fuel emplacement began, failures of several near-field instruments were observed at the SFT-C. Failures of linear potentiometers occurred on canister drift extensometers located 1.4 to 2.0 m from the heat sources. Failures of vibrating-wire stressmeters emplaced about 1 m from the heat source also occurred.

ROD EXTENSOMETER TRANSDUCER FAILURES

Extensometers of various types are used throughout the SFT-C.[3] The type of linear potentiometer which has failed is deployed in 14 four-anchor units in the canister drift (56 total), 12 three- and six-anchor units in the heater drifts (60 total), 7 three-component fracture monitors (21 total), 16 two-component convergence wires (32 total), and 2 one-component convergence wires (2 total). To date, failures have been limited to the first named units which, like the second named units, are manufactured by Terrametrics in Golden, Colorado. The failing components are rectilinear potentiometers manufactured by Bourns Instruments, Inc., Riverside, California. Subsequent to the initial failures, which were expressed as nonlinear changes in total resistance (RT), replacement Bourns potentiometers were acquired. These units expressed failure before being fielded, this time as linear changes in RT. Of 64 transducers acquired for replacement, 21 (or 33%) were found to have RT outside the 5 kΩ ±10% specification.

Extensive tests were conducted on both the original and replacement G-series potentiometers, but no definite cause of failure has been identified. Failures of a nonlinear nature are apparently associated with the presence of chemical vapors (possibly acetic acid) in the head assembly and with irregular surface texture of the resistive element. Hygroscopy of the resistive element has been observed to produce linear changes in RT and thus may be at least a contributing factor in both the linear and nonlinear failures.

Since no definite cause of failure was determined, we elected to replace the 48 GBE- and GCE-series transducers with four types of transducers. This will permit an evaluation of available transducers. Twelve each Bourns potentiometers, Vernitron potentiometers, Schaevitz DCDT, and Kaman electromagnetic proximeters have been installed and calibrated _in situ_. The four types of transducers will experience three different environments: natural air, dry nitrogen, and a slight vacuum, all with the head assembly cover on. The length of the Schaevitz transducer required lengthening of the head-assembly cover.

These units have only recently been installed; i.e., October to November 1981. Evaluation of their performance will be discussed in later reports. A currently unresolved issue is the determination of when the transducer and, hence, the data became invalid. Until we can make convincing arguments to the contrary, we are assuming that all data from the GBE- and GCE-series extensometers that have exhibited nonlinear changes in RT are erroneous. This represents a loss of data from 23 displacement measuring devices (13% of the total) during the initial 1-1/2 years of the test. Whether or not this gap in the near-field extensometer data can be filled depends on how well measurements from other instruments compare with calculations. If data analysis indicates the calculated and measured displacements and stresses agree throughout the facility, it will be reasonable to interpolate between zero-time values at the original installation and replacement-time values subsequent to transducer replacement, after normalizing the measurements with respect to the calculations. Additional analyses must be performed before implementing a specific interpolation scheme.

VIBRATING-WIRE STRESSMETER FAILURES

Also incorporated in the SFT-C instrumentation program are 18 vibrating-wire stressmeters (VWSM) produced by IRAD Gage, a division of Creare Products, Inc., Lebanon, New Hampshire. Since their installation in March 1980, 13 (or 72%) of the 18 gauges have failed.

Disassembly of several of the failed stressmeters quickly defined the failure mechanism. Moisture had induced corrosion of the vibrating wire to the extent that its vibration was mechanically damped. In some cases, the corrosion formed a bridge between the wire and the gauge body. The precise source of the moisture was elusive since the gauges were O-ring sealed, coated, and foamed in place in relatively dry holes. A new gauge seal was designed which permitted hermetic sealing and evacuation of the gauge body. This design should eliminate intrusion of water and should also reduce the likelihood that moisture is in the gauge body at the time of manufacture.

Nine of the new design gauges were installed 16 to 17 June 1981, and are currently functioning reliably. The remaining four failed units have not been replaced because they are interspersed with five gauges of the original design which are continuing to function normally.

Once again, it is not completely clear when the stressmeters and data became unreliable. The stressmeters tend to exhibit very erratic behavior just before final failure. On the other hand, gauges which ultimately failed showed a period of increasingly high readings before erratic behavior began (see Fig. 9). This suggests that corrosion can cause sufficient mass loading or weakening of the wire to markedly change its frequency without making the gauge erratic or unreadable. Periodic reading of the Q of the wire, using the MB-6 readout unit and oscilloscope, should resolve whether or not either mass loading or weakening of the wire is occurring as a precursor to failure. Since this was not done on the original stressmeters, we must conclude that all data from failed stressmeters are erroneous.

REFERENCES

1. L. D. Ramspott, L. B. Ballou, R. C. Carlson, D. N. Montan, T. R. Butkovich, J. E. Duncan, W. C. Patrick, D. G. Wilder, W. G. Brough, and M. C. Mayr, Technical Concept for a Test of Geologic Storage of Spent Reactor Fuel in the Climax Granite, Nevada Test Site, Lawrence Livermore National Laboratory, Livermore, CA, UCRL-52796 (1979).
2. D. N. Montan, Thermal Analysis for a Spent Reactor Fuel Storage Test in Granite, Lawrence Livermore National Laboratory, Livermore, CA, UCRL-83995 (1980), also in Proceedings of the International Symposium on the Scientific Basis for Nuclear Waste Management, Vol. 3 (1981).
3. W. G. Brough and W. C. Patrick, Instrumentation Report No. 1: Specification, Design, Calibration, and Installation of Instrumentation for an Experimental, High-Level Nuclear Waste Storage Facility, Lawrence Livermore National Laboratory, Livermore, CA, UCRL-53248 (1981).
4. R. C. Carlson, W. C. Patrick, D. G. Wilder, W. G. Brough, D. N. Montan, P. E. Harben, L. B. Ballou, and H. C. Heard, SFT-C Technical Measurements Interim Report FY1980, Lawrence Livermore National Laboratory, Livermore, CA, UCRL-53064 (1980).
5. W. C. Patrick and W. G. Brough, Response of Borehole Extensometers to Explosively Generated Dynamic Loads, Lawrence Livermore National Laboratory, Livermore, CA, UCRL-53087 (1980).
6. Personal communication, R. C. Carlson to M. Hughes, 25 September 1980.

LR

APPENDIX A

RESISTANCE AND SHAFT-LENGTH MEASUREMENTS FOR ORIGINAL G-SERIES POTENTIOMETERS

License No.	Serial No.	Total resistance (Ω) (13 Nov 79)	Total resistance (Ω) (19 Nov 80)	Wiper to end point resistance (Ω) (19 Nov 80) GRN-RD	Wiper to end point resistance (Ω) (19 Nov 80) YEL-RD	Shaft length (in.)
GAE011	3578-356	5138	5271	2641	2674	.644
GAE012	3578-357	5238	5332	2644	2715	.668
GAE013	3578-383	4943	5120	2540	2629	.636
GAE014	3578-359	5214	5348	2629	2749	.660
GAE010	VISHAY resistances = 2534 and 2498 Ω, Excitation = 10.551226 V					
GBE011	3578-360	5167	5341	2647	2732	.637
GBE012	3578-361	5207	5455	2647	2826	.662
GBE013	3978-561	5105	5989	2747	3385	.666
GBE014	3578-363	5130	5814	2643	3221	.664
GBE010	VISHAY resistances = 2500 and 2501 Ω, Excitation = 10.483574 V					
GBE021	3578-364	5292	6622	2821	3860	.666
GBE022	3578-365	5302	4950	2415	2598	.672
GBE023	3578-366	4848	20,810	3139	18,030	.685
GBE024	3578-367	4696	5311	2355	2992	.689
GBE020	VISHAY resistances = 2498 and 2580 Ω, Excitation = 10.495949 V					
GBE031	3578-368	4877	5322	2571	2798	.655
GBE032	3578-369	4876	5882	2537	3383	.653
GBE033	3578-370	4933	5516	2503	3061	.684
GBE034	3578-371	5416	10,011	3379	6683	.676
GBE030	VISHAY resistances = 2497 and 2498 Ω, Excitation = 10.493378 V					

License No.	Serial No.	Total resistance (Ω) (13 Nov 79)	Total resistance (Ω) (19 Nov 80)	Wiper to end point resistance (Ω) (19 Nov 80) GRN-RD	Wiper to end point resistance (Ω) (19 Nov 80) YEL-RD	Shaft length (in.)
GBE041	3578-372	5388	7920	2989	4967	.663
GBE042	3578-373	5048	5819	2670	3228	.658
GBE043	3578-374	4999	5304	2553	2797	.661
GBE044	3578-375	4941	10,551	2960	7915	.662
GBE040	VISHAY resistances = 2499 and 2499 Ω, Excitation = 10.514727 V					
GBE051	3578-376	5308	5989	2833	3201	.641
GBE052	3578-377	4927	5355	2561	2836	.650
GBE053	3578-378	5320	5493	2678	2890	.670
GBE054	3578-379	5327	11,220	2894	8377	.662
GBE050	VISHAY resistances = 2498 and 2498 Ω, Excitation = 10.512056 V					
GBE061	3578-380	5393	5635	2831	2859	.661
GBE062	3578-381	4753	4914	2465	2514	.650
GBE063	4078-026	4933	5124	2539	2641	.664
GBE064	4078-027	4744	5019	2476	2601	.649
GBE060	VISHAY resistances = 2499 and 2498 Ω, Excitation = 10.499895 V					
GCE011	3578-384	4791	4993	2476	2557	.651
GCE012	3578-385	5027	5197	2533	2702	.660
GCE013	3978-574	5002	5981	2755	3300	.670
GCE014	3978-337	4896	7825	2525	5370	.642
GCE010	VISHAY resistances = 2499 and 2507 Ω, Excitation = 10.468107 V					

License No.	Serial No.	Total resistance (Ω) (13 Nov 79)	Total resistance (Ω) (19 Nov 80)	Wiper to end point resistance (Ω) (19 Nov 80) GRN-RD	Wiper to end point resistance (Ω) (19 Nov 80) YEL-RD	Shaft length (in.)
GCE021	3978-338	4869	5041	2507	2580	.681
GCE022	3978-339	5022	5871	2675	3253	.683
GCE023	3978-340	4744	6500	REMOVED		
GCE024	3978-341	4728	2504	1896	2138	.655
GCE020	VISHAY resistances = 2500 and 2500 Ω, Excitation = 10.451056 V					
GCE031	3978-342	4747	5042	2520	2619	.656
GCE032	3978-554	4807	5024	2449	2637	.665
GCE033	3978-555	4674	4090	2422	1420	.671
GCE034	3978-556	4803	5081	2380	2757	.685
GCE030	VISHAY resistances = 2498 and 2498 Ω, Excitation = 10.450417 V					
GCE041	3978-557	4738	4981	2460	2580	.646
GCE042	3978-558	4930	5090	2513	2700	.644
GCE043	3978-559	5045	5499	2621	2928	.666
GCE044	3978-560	4718	5523	2574	3032	.689
GCE040	VISHAY resistances = 2502 and 2498 Ω, Excitation = 10.436565 V					
GCE051	4078-028	4863	5665	2739	2993	.672
GCE052	4078-029	4743	4966	2437	2573	.673
GCE053	4078-030	4813	6179	2656	3600	.654
GCE054	4078-031	4837	5017	2380	2682	.666
GCE050	VISHAY resistances = 2498 and 2509 Ω, Excitation = 10.453707 V					

License No.	Serial No.	Total resistance (Ω) (13 Nov 79)	Total resistance (Ω) (19 Nov 80)	Wiper to end point resistance (Ω) (19 Nov 80) GRN-RD	Wiper to end point resistance (Ω) (19 Nov 80) YEL-RD	Shaft length (in.)
GCE061	3978-565	5108	5245	2629	2675	.573
GCE062	3978-566	4734	4923	2419	2551	.659
GCE063	3978-567	5350	5107	2570	2570	.651
GCE064	3978-568	5099	5887	2689	3245	.690
GCE060	VISHAY	resistances = 2498 and 2500 Ω, Excitation = 10.450207 V				
GDE011	4078-032	4869	5253	2646	2658	.638
GDE012	4078-033	4706	5070	2596	2613	.651
GDE013	4078-034	5106	5239	2648	2647	.653
GDE014	4078-035	5094	5265	2644	2657	.649
GDE010	VISHAY	resistances = 2498 and 2499 Ω, Excitation = 10.440166 V				

Table B-1. Resistance measurements for MBI-series potentiometers.

License No.	Serial No.	Total resistance (Ω) (Nov 79)	Total resistance (Ω) (7 May 81)
MBI011	3978-570	4858	5068
MBI012	3978-571	4957	5174
MBI013	3578-330	5372	5435
MBI021	3578-412	4822	4887
MBI022	3578-413	5220	5316
MBI023	3578-414	N/A	5072
MBI024	3578-415	N/A	5193
MBI025	3578-511	N/A	5192
MBI026	3678-029	5113	5187
MBI031	3578-406	5299	5361
MBI032	3578-407	4729	4789
MBI033	3578-408	4958	5036
MBI034	3578-409	5460	5545
MBI035	3578-410	5003	5065
MBI036	3478-269	5272	5364
MBI041	3578-325	5023	5058
MBI042	3578-326	5380	5423
MBI043	3578-327	5099	5161
MBI051	3578-337	5085	5164
MBI052	3578-338	5164	5217
MBI053	3578-339	4994	5036
MBI054	3578-340	5152	5203
MBI055	3578-341	5265	5317
MBI056	3978-573	4602	4798

Table B-1. (Continued.)

License No.	Serial No.	Total resistance (Ω) (Nov 79)	(7 May 81)
MBI061	3578-392	4943	4997
MBI062	3478-270	4887	4988
MBI063	3578-394	4976	5031
MBI064	3578-395	5085	5144
MBI065	3578-396	5273	5318
MBI066	3578-397	4735	4763
MBI081	3578-389	5228	5034
MBI082	3578-332	5020	5045
MBI083	3578-333	5445	5466
MBI091	3578-386	4801	4881
MBI092	3578-387	5305	5425
MBI093	3578-388	5255	5351
MBI094	3578-391	5467	5538
MBI095	3578-390	5124	5249
MBI096	3478-268	5206	5356
MBI101	3978-569	4816	4945
MBI102	3978-562	4797	4973
MBI103	3578-346	5025	5125
MBI104	3578-347	5083	5195
MBI105	3578-348	4828	4953
MBI106	3578-349	5241	5326
MBI111	3478-267	4890	4998
MBI112	3578-335	5069	5112
MBI113	3578-336	5250	5282

Table B-1. (Continued.)

License No.	Serial No.	Total resistance (Ω) (Nov 79)	(7 May 81)
MBI121	3578-398	4858	4954
MBI122	3578-401	4835	4893
MBI123	3578-402	5009	5109
MBI124	3578-403	5235	5359
MBI125	3578-404	5154	5248
MBI126	3578-405	5050	5147
MBI131	3578-350	N/A	5330
MBI132	3578-351	5056	5116
MBI133	3578-352	4961	4950
MBI134	3578-353	5243	5306
MBI135	3978-563	5053	5179
MBI136	3978-564	5074	5253

Table B-2. Resistance measurements for CWE-, FMS-, and THE-series potentiometers.

License No.	Serial No.	Resistances (7 May 81) (Ω) RT	GRN-RED	YEL-RED	Vishay resistors (Ω)
CWE011	0680-414	4693	2506	2268	2501/2501
CWE012	0680-415	4845	2530	2348	2502/2499
CWE021	0680-416	4856	2546	2333	2501/2501
CWE022	0680-417	4982	2569	2472	2497/2501
CWE031	0680-418	5075	2721	2488	2503/2503
CWE032	0680-419	5070	2595	2531	2501/2501
CWE041	0680-420	5232	2792	2472	2502/2502
CWE042	0680-421	4733	2492	2283	2502/2502
CWE051	0680-422	4792	2529	2314	2503/2502
CWE052	0680-423	5290	2728	2628	2502/2501
CWE061	0680-424	5381	2874	2535	2499/2499
CWE062	0680-425	5015	2748	2310	2500/2501
CWE071	0680-426	4685	2524	2195	2499/2500
CWE072	0680-427	4913	2558	2387	2499/2499
CWE081	0680-428	5132	2855	2324	2500/2500
CWE082	0680-441	5300	2724	2632	2499/2501
CWE091	0680-442	5012	2816	2245	2499/2500
CWE092	0680-443	5203	2686	2545	2499/2500
CWE101	0680-444	5301	2963	2384	2500/2500
CWE104	0680-450	4973	2674	2373	2500/2500
CWE111	0680-447	4814	2575	2284	2499/2499
CWE112	0680-448	5072	2646	2473	2499/2500
CWE131	0680-454	5142	2655	2529	2500/2499
CWE132	0680-455	4994	2582	2480	2499/2499
CWE141	0680-456	5175	2719	2519	2500/2499
CWE142	0680-451	4867	2459	2443	2499/2499
CWE151	0680-458	5296	2763	2597	2499/2499
CWE152	0680-459	5057	2585	2503	2499/2499
CWE161	0680-460	5229	2749	2521	2499/2499
CWE162	0680-461	4746	2441	2347	2499/2499
CWE171	0680-463	4933	2580	2405	2499/2499
CWE172	0680-464	5137	2636	2551	2499/2499

Table B-2. (Continued.)

License No.	Serial No.	Resistances (7 May 81) (Ω) RT	GRN-RED	YEL-RED	Vishay resistors (Ω)
FMS011	0680-387	4929	2534	2561	1666
FMS012	0680-388	4993	2595	2496	1666
FMS013	0680-389	4714	2373	2371	1666
FMS021	0680-391	4985	2516	2528	1665
FMS022	0680-392	5050	2531	2563	1665
FMS023	0680-393	5441	2769	2748	1665
FMS031	0680-395	4973	2536	2481	1665
FMS032	0680-396	4763	2389	2419	1665
FMS033	0680-398	5109	2586	2598	1665
FMS041	0680-399	4738	2375	2379	1665
FMS042	0680-400	5110	2589	2610	1665
FMS043	0680-404	5102	2572	2565	1665
FMS051	0680-405	4847	2441	2460	1666
FMS052	0680-406	5129	2608	2571	1666
FMS053	0680-407	4981	2504	2513	1666
FMS061	0680-408	5086	2610	2531	1665
FMS062	0680-409	4951	2495	2484	1665
FMS063	0680-410	5317	2677	2691	1665
FMS071	0680-411	5053	2544	2538	1665
FMS072	0680-412	4922	2486	2469	1665
FMS073	0680-413	4854	2469	2469	1665
THE020	0680-385	4818	2582	2296	2499/2499
THE030	0680-386	4980	2652	2379	2499/2499

Note: FMS Vishay resistor reading is parallel set.

APPENDIX C

RESISTANCE MEASUREMENTS FOR REPLACEMENT G-SERIES POTENTIOMETERS

Serial No.	Date of receipt	Total Resistance (Ω) On day of receipt	On 21 April 1981	On 28 July 1981
4078-005	4 Jan 80	5084	5639	N/A
4078-006	3 Jan 80	4798	4870	4838
4078-007	4 Jan 80	4858	5125	5020
4078-008	4 Jan 80	4880	5040	4935
4078-009	4 Jan 80	5035	5510	5398
4078-010	4 Jan 80	4781	4750	4877
4078-011	4 Jan 80	4839	5120	5107
4078-013	4 Jan 80	4986	5323	5061
4078-015	4 Jan 80	4838	4816	4881
0581-502	8 Apr 81	4807	4802	4813
0581-504	9 Apr 81	4929	5120	5063
0581-516	8 Apr 81	5036	5028	5034
1780-145	8 Apr 81	4931	4924	4927
1780-155	8 Apr 81	4920	6038	N/A
1780-159	8 Apr 81	5169	5251	5264
4880-223	9 Apr 81	5046	5522	5546
4480-449	9 Apr 81	4908	4911	4918
4480-453	9 Apr 81	5169	6127	5567
4480-455	8 Apr 81	5169	5222	5227
4480-463	8 Apr 81	5256	5325	5340
4480-469	9 Apr 81	5058	5747	5402
0581-505	7 Apr 81	5285	4976	4981
0581-508	8 Apr 81	4731	4729	4740
0581-512	8 Apr 81	5200	5129	5203
0581-513	31 Mar 81	4943	5887	5377
1780-141	8 Apr 81	4983	4735	4741
1780-142	7 Apr 81	4877	4855	4857

Serial No.	Date of receipt	Total Resistance (Ω) On day of receipt	On 21 April 1981	On 28 July 1981
1780-144	8 Apr 81	4805	5242	4955
1780-147	8 Apr 81	4983	4780	4774
1780-148	8 Apr 81	4947	5497	5194
1780-149	30 Mar 81	5115	5291	5417
1780-156	27 Mar 81	5012	5009	N/A
5280-335	27 Mar 81	4917	8067	N/A
0581-503	27 Mar 81	4727	4815	4857
0581-506	27 Mar 81	4834	4833	N/A
0581-517	27 Mar 81	4994	5016	5026
1780-150	27 Mar 81	5173	5185	5189
1780-154	27 Mar 81	5104	5750	5681
4880-221	27 Mar 81	5393	5464	5476
4880-229	27 Mar 81	5284	5310	5322
4480-459	27 Mar 81	5271	5297	5308
4480-461	27 Mar 81	5176	5298	5307
4480-464	27 Mar 81	5085	5232	5240
4480-465	27 Mar 81	4667	4665	4673
4480-467	27 Mar 81	5269	5560	5464
0581-507	27 Mar 81	5086	7962	6199
0581-511	27 Mar 81	4802	5140	4971
0581-515	27 Mar 81	5086	5412	5260
1780-158	27 Mar 81	4827	5047	4940
1780-146	27 Mar 81	5179	4944	4911
4480-446	27 Mar 81	5234	6743	6145
4480-450	27 Mar 81	5216	6851	6162
4480-452	27 Mar 81	5219	6198	5782
4480-456	27 Mar 81	5014	7448	6458
4480-457	27 Mar 81	4891	6495	5569
4480-458	27 Mar 81	5217	5517	N/A
4480-460	27 Mar 81	5130	5218	5206
0581-514	27 Mar 81	4906	4903	4913
4880-224	27 Mar 81	4961	5523	5307

Serial No.	Date of receipt	Total Resistance (Ω) On day of receipt	On 21 April 1981	On 28 July 1981
4880-225	27 Mar 81	5017	5980	5436
4480-466	27 Mar 81	4735	5283	5297
4480-468	27 Mar 81	4922	6592	5583
5280-330	27 Mar 81	4756	4968	4859
5280-332	27 Mar 81	5123	6917	5738

Note: N/A indicates not available because of use in evaluation.

U.S. Government Printing Office: 1982/6-587-055/29